

DR.JIT: A Just-In-Time Compiler for Differentiable Rendering

WENZEL JAKOB, École Polytechnique Fédérale de Lausanne (EPFL), Switzerland
 SÉBASTIEN SPEIERER, École Polytechnique Fédérale de Lausanne (EPFL), Switzerland
 NICOLAS ROUSSEL, École Polytechnique Fédérale de Lausanne (EPFL), Switzerland
 DELIO VICINI, École Polytechnique Fédérale de Lausanne (EPFL), Switzerland

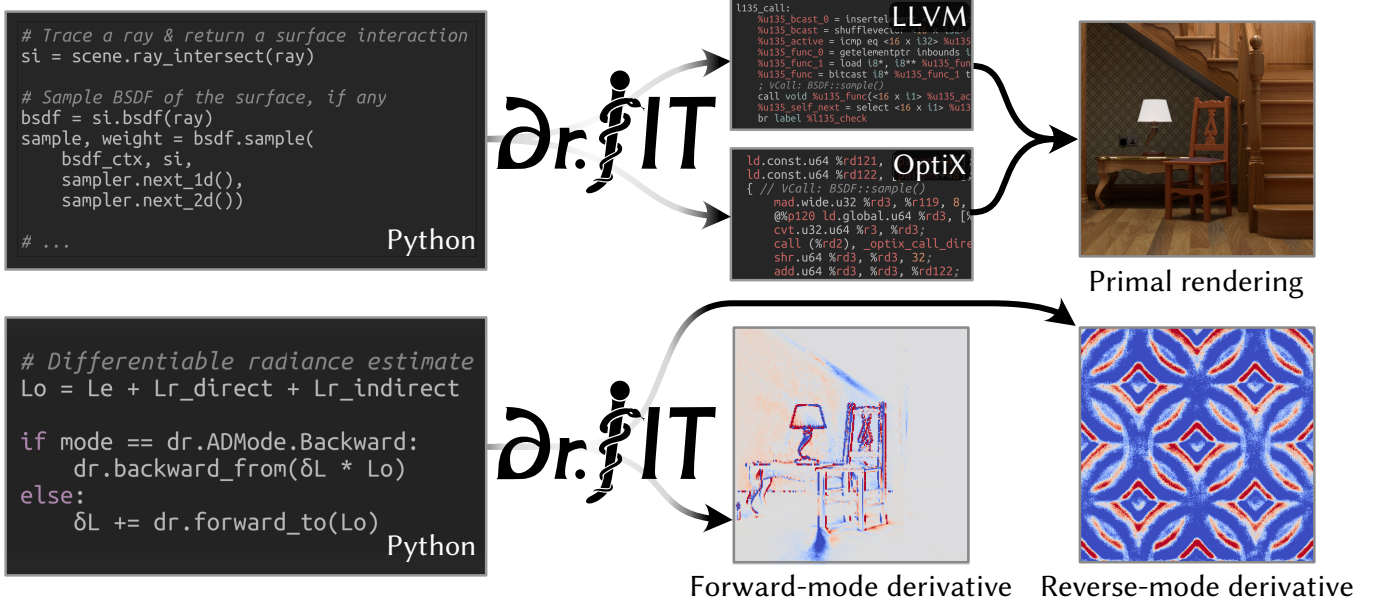


Fig. 1. DR.JIT is a domain-specific compiler for physically-based (differentiable) rendering. When DR.JIT executes a rendering algorithm, it generates a *trace*: a large computation graph comprising all interaction between the rendering algorithm and scene objects like shapes, BSDFs, textures, and emitters. It compiles this graph representation into a CPU- (via LLVM) or GPU- (via OptiX) megakernel, producing efficient specialized code for the provided scene. In benchmarks comparing its performance to Mitsuba 2 and PBRT 4 on the GPU, it achieves geometric mean speedups of 2.66x and 1.64x, respectively. Besides compilation, DR.JIT also provides an expressive automatic differentiation system tailored to the needs of differentiable rendering. It supports both forward- and reverse-mode differentiation: the former visualizes a perturbation in image space, which is mainly helpful for debugging and visualization. The latter provides derivatives in parameter space (e.g. texels of the wallpaper) and enables simultaneous optimization of large numbers of unknowns.

We present DR.JIT, a domain-specific just-in-time compiler for physically based rendering and its derivative. DR.JIT traces high-level programs (e.g., written in Python) and compiles them into efficient CPU or GPU megakernels. It achieves state-of-the-art performance thanks to global optimizations that specialize code generation to the rendering or optimization task at hand.

While DR.JIT drastically simplifies the creation of fast Monte Carlo renderers, its design was motivated by the needs of the differentiable rendering community. Builtin facilities for automatic differentiation expose fine-grained control over subtle details of the differentiation process needed to transform the derivative of a simulation into a simulation of the derivative, a prerequisite for high performance in this context. Just-in-time compilation embraces the dynamic nature of gradient evaluation: only small portions of the renderer may need derivative tracking in a specific task, but their location cannot be known ahead of time. Our system specializes algorithms on the fly and removes detected redundancies.

Authors' addresses: Wenzel Jakob, École Polytechnique Fédérale de Lausanne (EPFL), Switzerland, wenzel.jakob@epfl.ch; Sébastien Speierer, École Polytechnique Fédérale de Lausanne (EPFL), Switzerland, sebastien.speierer@epfl.ch; Nicolas Roussel, École Polytechnique Fédérale de Lausanne (EPFL), Switzerland, nicolas.rousseau@epfl.ch; Delio Vicini, École Polytechnique Fédérale de Lausanne (EPFL), Switzerland, delio.vicini@epfl.ch.

CCS Concepts: • Software and its engineering → Just-in-time compilers; • Mathematics of computing → Automatic differentiation; • Computing methodologies → Rendering.

1 INTRODUCTION

Recent progress in the area of *physically based differentiable rendering* (henceforth “PBDR”) has produced methods that can differentiate light transport and scattering with respect to arbitrary scene parameters, enabling the solution of nonlinear problems involving large sets of unknowns. Diverse scientific and engineering disciplines require this type of inverse analysis and stand to benefit from these developments.

While the theory of PBDR continues to evolve, practical aspects of these methods have remained a persistent challenge. For example, the reverse-mode derivative of a conceptually simple algorithm like path tracing [Kajiya 1986] with precautions for linear-time complexity [Vicini et al. 2021] and unbiased visibility handling [Bangaru et al. 2020] turns into an enormously complex function. Leaving efficiency aside, merely producing a correct implementation of such

a large and intricate program is near-impossible even for experts in the field. Correctness alone is also unsatisfactory: optimizations tend to run for thousands of iterations, hence the resulting program also needs to be fast. It is evident that better tools are needed to simplify development and bridge this conspicuous gap between PBDR theory and practice.

Rendering is not alone with these needs, and a number of highly relevant tools have been developed during the last decades. For example, methods for *automatic differentiation* (AD) can completely eliminate the tedious process of manual differentiation. In recent years, keen interest in machine learning has precipitated the development of numerous frameworks and programming languages for differentiable array programming that combine AD with n -dimensional array representations. They are an appealing choice for many optimization problems and indeed tend to be highly effective when the problem at hand is naturally expressible in terms of the available array operations. It would seem that the article could simply end here: the rendering algorithm should then be implemented on top of such a framework, which will provide all of the desired derivatives. However, several characteristics of rendering are unusual in the array programming setting, which means that PBDR workloads either fall off the fast path or cannot be represented at all.

The first is the use of *subtype polymorphism*, in which an instance of one type can masquerade as another type. Rendering algorithms build on this concept to dynamically dispatch method calls from abstract component interfaces to concrete implementations. We show how the ability to represent, differentiate, and optimize polymorphic constructions is instrumental for good performance in both ordinary (henceforth “primal”) and differential rendering phases.

A second difference is the organization of the computation into parallel phases known as *kernels*. Compilers for array programs like XLA [Google 2017] analyze the graph structure of the desired computation, *fusing* operations into kernels via *just-in-time* (JIT) compilation as part of a heuristically guided clustering process. This often boils down to selecting among the thousands of vendor-tuned kernels included in libraries like NVIDIA’s cuDNN [Chetlur et al. 2014] or Apple’s Metal Performance Shaders [Apple, Inc. 2021]. The arithmetic intensity of these kernels is high enough that the cost of inter-kernel communication is normally not the dominating factor.

In contrast, partitioning the computation performed by a rendering algorithm into multiple kernels comes at a *significant cost* due to the large amount of memory traffic that is then necessary to exchange Monte Carlo sample data. We find that it is almost always preferable to reduce communication to a minimum by performing the bulk of the computation within a single *megakernel*. However, compiling rendering software into megakernels is nontrivial, and recent *wavefront*-style rendering systems like *PBRT 4* [Pharr et al. 2020] and *Mitsuba 2* [Nimier-David et al. 2019] have eschewed them for this reason. Our dynamic compilation approach can map high-level rendering code to different granularities of wavefronts and megakernels, enabling a closer investigation of the performance spectrum of different implementations. Compared to a wavefront baseline, Dr.JIT accelerates our experimental workloads by a factor of $13.7\times$ (geometric mean) while consuming $82\times$ less memory.

A third difference between rendering and other domains is that the direct application of AD to a primal algorithm is almost never

desirable: not only does this lead to extremely inefficient derivative code, but it also produces gradients that are so severely biased that they normally cannot be used for optimization. State-of-the-art PBDR methods exploit physical reciprocity [Nimier-David et al. 2020] and arithmetic invertibility [Vicini et al. 2021] to transform the derivative of a simulation into a simulation of the derivative. They dynamically adapt the parameterization of Monte Carlo integrals to address bias arising from the discontinuous visibility function [Loubet et al. 2019; Bangaru et al. 2020]. All of these steps require unusually fine-grained control over AD at the inner loop of the renderer.

We present Dr.JIT, a just-in-time compiler that addresses these and related needs of the rendering research and differentiable rendering communities. Dr.JIT traces high-level programs (typically written in the Python language) and compiles them into efficient megakernels for diverse architectures. Its GPU backend generates OptiX [Parker et al. 2010] programs that leverage ray tracing hardware acceleration, while a separate CPU backend generates vectorized code for various processor architectures building on the LLVM compiler infrastructure [Lattner and Adve 2004]. The generated code is specialized to the problem at hand and can, e.g., only render or optimize a specific scene, but this also enables a range of useful optimizations. A fundamental design constraint of the system is that the use of high-level constructs like AD, ray tracing, polymorphism, and loops *must never* break up the megakernel due to the large inter-kernel communication overheads that this would imply.

We also highlight two directions that are *not* goals of our system: first, Dr.JIT is not a general-purpose array programming tool, and performance on such workloads will be inferior to existing solutions. Second, while Dr.JIT greatly simplifies the design of PBDR methods, it does not free the developer from thinking about subtle details of the differentiation process. It enables—but does not automate—the introduction of the previously mentioned “reversibilities” (physical, mathematical) to improve efficiency when transforming ordinary rendering algorithms into differentiable counterparts. Automating such advanced program transformations is interesting but beyond the scope of this article.

Following a review of prior work, we discuss problem-specific constraints and central decisions that have shaped the design of Dr.JIT, covering compilation (Section 3) and differentiation (Section 4) in turn. Our experimental evaluations investigate both primal rendering and two state-of-the-art PBDR algorithms—their Python implementation is provided in the paper’s supplemental material to provide a concrete example of the high-level development style that Dr.JIT enables.

2 RELATED WORK AND BACKGROUND

2.1 Automatic Differentiation

Manual differentiation of mathematical expressions is error-prone and mechanical. The natural desire to delegate this task to a computer began with pioneering work in the 1950s and 1970s [Nolan 1953; Wengert 1964; Linnainmaa 1976] followed by comprehensive study in the 1980s [Speelpenning 1980; Griewank et al. 1989]. Griewank and Walther’s book [2008] reviews what has been learned about AD over the course of these many decades.

Given the consolidated understanding of the mathematical structure and asymptotic complexity of various derivative propagation strategies, there is a surprising degree of variety when it comes to how AD should be exposed to the user. The space of methods includes tracing, source-to-source transformation of abstract syntax trees or lowered *intermediate representations* (IR), and hybrids combining tracing with transformation. Differentiation can target scalar and dense or sparse array programs in forward, reverse-, and mixed modes, computing gradients or potentially higher-order derivatives of pure and impure functions. Covering all techniques in detail is far beyond the scope of this paper, and we refer to a recent survey by Baidin et al. [2018]. Here, we mainly cover the core concepts, noteworthy related methods for first-order derivatives, and their relationship to our approach.

Directionality. The main high-level flavors of AD are the *forward* and *reverse* (also known as *adjoint* or *backward*) modes. Forward mode evaluates a *Jacobian-vector-product* (often abbreviated “JVP”) of the form $\delta y = J_f \delta x$, where J_f is the Jacobian of the primal computation $y = f(x)$ and reverse mode evaluates a *vector-Jacobian-product* (“VJP”) of the form $\delta x = \delta y^T J_f$. Both can in principle compute the same derivatives, but forward mode does this more efficiently when the function being differentiated has few inputs (ideally just one), while reverse mode is efficient if it has few outputs. Realistic scene descriptions have million of unknowns, hence practical usage of differentiable rendering depends on reverse mode.

Reverse mode. The key issue with reverse mode is that it inverts the data dependencies of the original program. The derivative of this reversed program references intermediate steps of the primal calculation, which raises the age-old question of how they should be obtained. Exhaustive storage is simple but does not scale, as modern processors can generate many terabytes of intermediate state per second. The usual remedy is to only store this state at a sparse set of *checkpoints* with later recovery via reevaluation from the nearest one [Volin and Ostrovskii 1985]. Automatic recursive usage of this pattern reduces storage and runtime overheads of a program with t operations to a factor of $O(\log t)$ [Siskind and Pearlmutter 2018].

Adjoint. Whenever possible, *custom adjoints* are preferable to checkpointing. This refers to differentiation techniques that exploit problem-specific traits to alleviate or completely remove storage and reevaluation overheads. For example, differentiating through all iterations of a multivariate Newton’s method would be unnecessarily inefficient; it is far better to invoke the implicit function theorem that directly extracts all derivatives from the iteration’s fixed point. Similarly, the solution of an ordinary differential equation (ODE) admits an efficient adjoint that integrates the ODE backwards in time [Pontryagin 1962].

Adjoint for rendering. Light transport simulations also admit efficient custom adjoints: *Radiative Backpropagation* (RB) [Nimier-David et al. 2020] exploits physical reciprocity to transform the derivative of a simulation into another simulation that replaces radiance and importance by *derivative radiation* termed differential and adjoint radiance. An issue of the unbiased form of RB is that it must re-evaluate the primal radiance during derivative propagation, which incurs a runtime cost of $O(n^2)$ for light paths of length n .

Path Replay Backpropagation (PRB) [Vicini et al. 2021] builds on RB and furthermore exploits the mathematical invertibility of certain steps of the computation to recover the primal radiance on the fly.

Tracing. Assuming that efficient adjoints are available, the next important question is how the computation to be differentiated should be ingested by the AD system. Methods based on *tracing* record an evaluation trace (also referred to as a *Wengert tape* or *computation graph*) of all differentiable arithmetic operations; differentiation traverses this trace once more to propagate derivatives in forward or reverse mode. Control flow constructs are elided in the trace, which thus contains unrolled versions of all loops and taken branches. Tracing has seen widespread adoption through tools like PyTorch [Paszke et al. 2017], in which a typical neural network produces a trace with at most a few hundred high-level array operations. The reverse-mode sweep then invoke efficient adjoints of each operation. Tracing inherits the usual caveats of reverse mode—for example, differentiating long-running loops can be challenging. It also adds runtime overheads that can normally be amortized when differentiating array programs, but they dominate in *scalar programs* that manipulate individual floating point values. In iterative computations, tracing is often performed repeatedly, which causes further overheads and inhibits optimization.

Source transformation. AD via *source transformation* converts a source-level specification of a program into its derivative. In essence, differentiation becomes a compilation step, which turns AD overheads into a one-time cost and therefore also makes efficient derivatives of scalar programs possible.

Figure 2 illustrates this on a (not particularly good) implementation of an integer power x^n function, with JVP/VJP variants generated by Tapenade [Hascoet and Pascual 2013]. A key advantage of source transformation is the preservation of control flow: unlike an

```
def pow(x: float, n: int):
    y = 1
    for i in range(n):
        y *= x
    return y

def pow_jvp(x, n, dx):
    y = 1
    dy = 0
    for i in range(n):
        dy = x*dy + y*dx
        y *= x
    return dy

def pow_vjp(x, n, dy):
    y = 1
    dx = 0
    stack = []
    for i in range(n):
        stack.append(y)
        y *= x
    for i in reversed(range(n)):
        y = stack.pop()
        dx += y*dy
        dy *= x
    return dx
```

Fig. 2. Derivatives of a program obtained using *source transformation*. Here, `pow` raises x to the n -th power ($n \in \mathbb{N}$). The JVP/VJP versions were generated by Tapenade [Hascoet and Pascual 2013] and translated to Python. Both require the primal function arguments as input. The JVP further takes the function input derivatives and converts them into output derivatives, while the VJP takes output derivatives and converts them into input derivatives.

unrolled trace, the programs in Figure 2 remain usable regardless of the value of n (which controls the number of loop iterations).

Loops continue to be a nuisance, however: observe how the VJP requires two of them: the first records all intermediate loop state into a stack variable that is later consumed by a reversed loop. This poses difficulties on massively parallel architecture like GPUs: stack or *shadow memory* must be provisioned for all threads running in parallel, while handling worst-case requirements that are generally unknown. Note that pow only has a single differentiable argument and return value, hence JVP and VJP are in fact equivalent.

Curiously, certain optimizations that are trivial in one AD approach can become relatively difficult in another. For example, only a small subset of program variables usually affects the final gradient; it is desirable that the AD system recognizes this to avoid unnecessary evaluation of adjoints. In tracing AD, this optimization happens automatically because traversal along data dependencies cannot reach irrelevant variables. To achieve the same goal, source transformation tools must perform an *activity analysis* [Bischof et al. 1992; Hascoet and Pascual 2013], which is a data-flow analysis that conservatively propagates derivative liveness through the control flow graph until reaching a fixed point.

Four notable source transformation tools are Tapenade [Hascoet and Pascual 2013], Stalin ∇ [Pearlmutter and Siskind 2008], Zygote [Innes 2019], and Enzyme [Moses and Churavy 2020; Moses et al. 2021]. Tapenade uses sophisticated data-flow analyses to track activity, liveness, and numerous other optimization-relevant quantities in scalar C or Fortran programs involving pointers and array mutation. Stalin ∇ operates on λ -calculus IR and performs source-to-source transformations using runtime reflection. The *callee-derives* approach in their work shares some of the motivation of DR.JIT’s specialization of polymorphic derivatives. Zygote operates on typed IR of the Julia language and composes higher-level adjoints, while Enzyme differentiates code following lowering to LLVM IR. As with optimizing compilers, the IR’s abstraction level can either facilitate or exacerbate certain tasks, hence the suitability of these tools will depend on nature of the problem to be differentiated.

Hybrid systems. Finally, we note that tracing and source transformation are merely the extreme points of a much larger space of *hybrid* techniques covering a wide spectrum of engineering trade-offs. For example, PyTorch [2017] programs can be traced into a domain-specific language for subsequent compilation, which removes tracing overheads and enables systematic optimization.

Jax [Bradbury et al. 2018] traces functions into an expressive IR and provides transformations to differentiate, parallelize, and compile this representation. Compilation proceeds via lowering into XLA [Google 2017] that applies tensorial optimizations like fusing sequences of matrix-vector multiplications into matrix-matrix multiplications and clustering the computation into a mix of vendor-provided and JIT-compiled kernels running on the CPU, GPU, or TPU. Jax also uses a highly related mechanism for loop tracing.

DR.JIT is also a hybrid in this classification: it traces differentiable arithmetic that is subsequently JIT-compiled at the function level to generate a megakernel with preserved control flow including loops and polymorphism.

2.2 Graphics and compilers

Graphics applications have a near-insatiable thirst for floating point operations, usually operating at the edge of what is possible on present hardware. These needs are often not well-served by existing programming languages and compilers, which has motivated the design of performance-focused systems and languages with broad impact. For example, following increased programmability of GPUs through languages like Cg [Mark et al. 2003], the *Brook* [Buck et al. 2004] project was instrumental in establishing their widespread use for general-purpose computation.

Hanrahan and Lawson [1990] proposed an early language for *shading* computation that proved highly influential in both offline and realtime rendering worlds. *SMASH* [McCool et al. 2002] introduced the idea of metaprogramming shaders by tracing arithmetic in a host language, and *Sh* [McCool et al. 2004] built on these ideas to facilitate specialization while performing optimizations like dead code elimination and constant propagation. He et al. [2016] proposed a system to rapidly explore shader optimization choices for rasterization rendering, later extending the underlying language to allow for improved modularity [He et al. 2018].

Development of simulators for fluid or rigid/deformable body motion is often hampered by the intertwined complexity of simulation code, data structures, and parallelization. *Ebb* [Bernstein et al. 2016] employs a relational data model to isolate these aspects, while generating efficient CPU/GPU implementations. The *Taichi* [Hu et al. 2019b] language targets simulations that operate on sparsely organized data and also provides numerous compilation backends.

Halide [Ragan-Kelley et al. 2013] simplifies the design of image processing pipelines by separating computation and *schedule*, which encompasses placement, parallelization, vectorization, and blocking.

Interest in gradient-based optimization has motivated extensions of these systems. A differentiable extension of *Halide* [Li et al. 2018] enables end-to-end optimization of image processing pipelines. The predictable structure of the underlying stencils enables highly effective optimizations (scatter-gather conversion) during differentiation. *DiffTaichi* [Hu et al. 2019a] endows *Taichi* with an efficient differentiation operator that preserves the megakernel structure of the simulation code. DR.JIT and *DiffTaichi* target different types of programs, but they share this high-level objective.

The *ISPC* vectorizing compiler [Pharr and Mark 2012] is widely used to accelerate graphics systems on the CPU, e.g. to implement vectorized wavefronts in the *MoonRay* production renderer [Lee et al. 2017]. The *Manuka* rendering architecture [Fascione et al. 2018] uses LLVM to JIT-compile shader graphs into vectorized implementations that execute in a parallelized batch shading phase. *Rodent* [Pérard-Gayot et al. 2019] builds on the *AnyDSL* [Leißa et al. 2018] partial evaluation framework and JIT-compiles specialized renders for each scene, sharing some of the motivation of DR.JIT.

Mitsuba 2 [Nimier-David et al. 2019] consists of generic specifications of rendering algorithms and scene objects that can be retargeted to address specific needs including differentiation, vectorization, spectral rendering, and polarization. These transformations are performed by an underlying library named *Enoki* [Jakob 2019], which also implements wavefront-style execution. DR.JIT was designed as a drop-in replacement for Enoki, which made it possible to

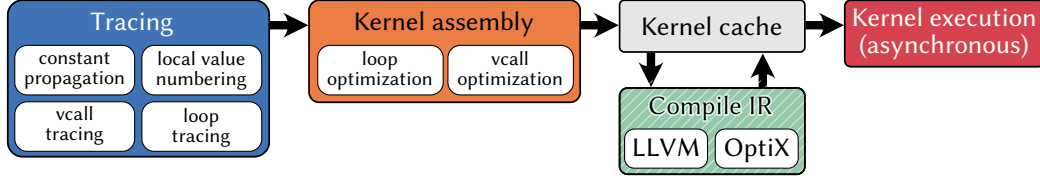


Fig. 3. The five main phases of DR.JIT. *Tracing* executes a Python or C++ program using custom arithmetic types that record operations into a graph data structure. Basic optimizations remove redundancies and reduce the size of the program. Tracing of loops and polymorphic constructs (virtual method calls) requires special precautions at this stage. *Kernel assembly* removes redundancies at a global level and produces a program in the desired intermediate representation (LLVM IR or PTX). Tracing and kernel assembly are highly optimized (on the order of 1-15ms in typical cases). A subsequent backend compilation step converts the generated IR into executable machine code. Backend compilation is relatively costly, hence DR.JIT consults an in-memory and on-disk kernel cache to see if this computation was previously encountered. Caching is a good fit for the repetitive computation produced by gradient-based optimizers.

experiment with compilation and differentiation while leveraging the infrastructure of an existing renderer.

Rendering algorithms evaluate integrals of discontinuous functions, which leads to severe issues with bias when these programs are later differentiated. We reparameterize [Loubet et al. 2019; Bangaru et al. 2020] integrals to address this problem. Other recent work has investigated specialized languages with builtin differentiation and integral operators that correct for such bias [Bangaru et al. 2021]. This approach requires finding all visible discontinuities in each computed integral (each triangle edge is a candidate), which runs into scalability issues in the context of PBDR.

NVIDIA OptiX [Parker et al. 2010] is a domain-specific compiler for programs using ray tracing. It analyzes the control flow graph and placement of ray tracing operations and partitions the program into a finite state machine, whose nodes exchange *continuation state* representing live variables. Recent hardware by NVIDIA offloads ray tracing steps to dedicated hardware cores. DR.JIT compiles GPU programs using OptiX, which requires conforming to its relatively strict execution model.

Laine et al. [2013] studied the performance of wavefront- and megakernel-style rendering and observed that complex GPU megakernels paradoxically often run more slowly than their communication-intensive wavefront counterparts. DR.JIT can generate both megakernels and wavefronts, which permits easy comparison between both approaches. Nearly a decade and four hardware generations later, we find that megakernels seem to have gained the upper hand.

3 JUST-IN-TIME COMPILATION

We now turn to DR.JIT’s computational substrate and postpone most discussion of differentiation to Section 4. Any use of the term *tracing* in this section thus refers to capturing computation for later compilation and is unrelated to AD.

DR.JIT is designed as a compatible replacement of the *Enoki* [Jakob 2019] library underlying *Mitsuba 2* [Nimier-David et al. 2019], which implies certain high-level similarities regarding the approach used to trace computation; differences between these tools will be discussed at the end of the section.

Figure 3 illustrates the high-level pipeline: following tracing, kernel assembly generates an IR representation requiring further backend compilation into machine code. In typical PBDR usage, this is only necessary during the first optimization iteration. The final

pipeline step launches the kernel for asynchronous execution on the CPU (via a thread pool) or the GPU (via CUDA/OptiX) so that tracing and kernel execution can continue in parallel.

We will now walk through the implementation of a simple *ambient occlusion* integrator and use this as an opportunity to introduce major system components, starting with low-level details and then progressively zooming out. Our program begins by importing¹ DR.JIT along with a floating point and an integer type.

```
import drjit as dr
from drjit.cuda import Float, UInt32
```

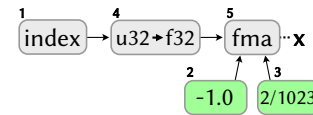
While types like `Float` and `UInt32` are suggestive of an internal scalar representation, they represent dynamically sized 1D arrays. Instances of them are best thought of as a scalar variable declaration within a loop of the form “`for index in range(...)`”, where `index` will usually refer to the Monte Carlo sample being computed.

Operations involving these capitalized types become part of the trace, while builtin Python types (`float`, `int`) and control flow statements are invisible to DR.JIT. In other words, this is a *metaprogram*, whose execution determines what computation will eventually take place on the target device.

The next line creates a `Float` variable containing 1024 evenly spaced numbers covering the interval `[-1, 1]` that we will shortly use to generate primary camera rays.

```
x = dr.linspace(Float, -1, 1, size=1024)
```

The trace of this expression consists of five variables: the aforementioned loop `index` variable, an int-to-float cast, and a *fused multiply-add* (FMA) referencing two *literal constants* shown in green:



A variable trace usually contains at least one use of the `index` variable (otherwise it is uniform.) Each temporary/variable is identified by a number (`x` points to `#5`); an associative data structure maps this index to a record describing the operation and its dependencies.

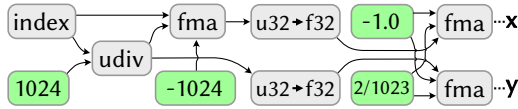
¹The shown source code fragments use the Python language, but the system is also usable via a near-identical C++ API. JIT-compilation and differentiation usually trace combinations of code written in both languages. Operations like `linspace` and `meshgrid` imitate their eponymous counterparts in other array programming tools.

The next step of our example creates another 1D array and invokes `dr.meshgrid` to expand both arrays into 2D grid coordinates.

```
y = dr.linspace(Float, -1, 1, size=1024)
x, y = dr.meshgrid(x, y)
```

Several points are worthy of note: the computation of the `y` variable is of course redundant. DR.JIT detects this using *local value numbering*, an optimization that uses the variable details (operation type, input dependencies) as *key* to query an auxiliary *inverse* version of the associative mapping. If an equivalent variable exists, it will be reused. The system also performs constant folding/propagation and basic algebraic simplifications (e.g. `fma(a, b, 0) = a*b; a*1=a`) while tracing. These optimizations are not important in our example, but they are highly effective in combination with AD that tends to generate many operations of this type. Both steps are cheap to do while tracing, and they can substantially reduce the size of the IR passed to OptiX/LLVM.

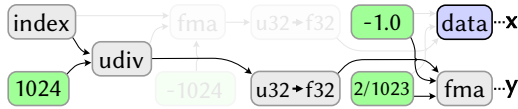
The function `dr.meshgrid()` computes row and column indices and then invokes `dr.gather()` to read from the two input arrays `x` and `y`. Both represent computation that has not occurred yet, hence `dr.gather` clones their graph representation with a rewritten index. Along with the previously mentioned optimizations, this produces



Suppose that the example takes place in an interactive session, and the user wishes to check the contents of the `x` variable at this point.

```
>>> print(x)
[-1.0, -0.998, -0.996, .. 1048570 skipped .., 0.996, 0.998, 1.0]
```

Accessing array contents triggers evaluation via `dr.eval(...)`, which compiles and launches a fused kernel that commits the requested variable(s) to device memory. Further use of `x` references the stored version, hence parts of the trace that are no longer needed expire.



We are now almost ready to trace a set of primary rays, using the 2D grid as image-space offsets in an orthographic camera model:

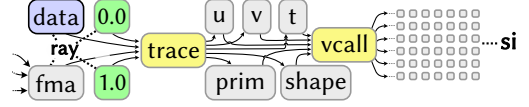
```
from mitsuba.core import Ray3f, Point3f, Vector3f, load_file
ray = Ray3f(o=Point3f(x, y, 0), d=Vector3f(0, 0, 1))
scene = load_file('scene.xml')
si = scene.ray_intersect(ray)
```

Our modified version of Mitsuba 2 uses DR.JIT-provided types throughout all interfaces; static vectorial types like `Point3f` simply wrap several JIT variables that become part of the generated program. The ray tracing operation requires further elaboration: its implementation looks as follows:

```
class Scene: # .. (most definitions omitted) ..
    def ray_intersect(self, ray: Ray3f) -> SurfaceInteraction3f:
        pi = self.ray_intersect_preliminary(ray)
        return pi.shape.compute_surface_interaction(pi)
```

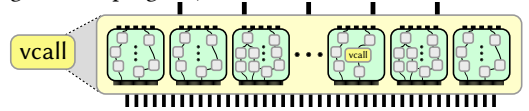
It first finds a *preliminary intersection* that consists of the intersected shape, primitive ID, ray depth and UV coordinates (our example

is simplified here to hide complexities like instancing). The second step invokes a method on the intersected shape (`pi.shape`) so that it can refine this preliminary intersection into a detailed `SurfaceInteraction3f` type describing the differential geometry at the intersection point. Within DR.JIT, this refined intersection maps to a large number of variables (41-45 depending on the variant of the renderer). Following these last steps, the trace looks as follows (repeated parts on the left are omitted):



The yellow color indicates complex operations with custom code generation hooks. During kernel assembly, `trace` compiles into IR operations that invoke a ray tracing accelerator (Embree [Wald et al. 2014] on the CPU, OptiX [Parker et al. 2010] on the GPU).

The `pi.shape` member of the preliminary intersection refers to an (as of yet unevaluated) array of 1024×1024 pointers to arbitrary shape implementations. The `vcall` variable represents the dynamic dispatch step (*virtual function call* in C++ terminology) needed to resolve the polymorphic nature of this operation. DR.JIT does so by tracing *all reachable* method implementations (scene objects register themselves with DR.JIT to enable this). The `vcall` variable can thus be interpreted as a large-scale demultiplexer-multiplexer that routes arguments and return values to/from instances. During kernel assembly, it produces IR performing an indirect branch to one of multiple subroutines (in other words, the indirection is preserved in the generated program).



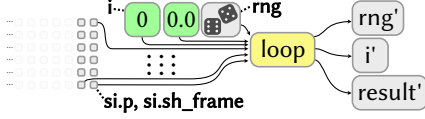
Several inefficiencies may be apparent to the reader at this point; we will soon explain how they are resolved. The final part of our example instantiates a loop that traces 128 ambient occlusion rays starting at the intersected position. For this, we require a random number generator and a looping mechanism. While a routine Python `for` loop works, it would unroll the loop body 128 times and produce an unnecessarily large trace. As before, it is desirable that tracing preserves the structure of the input program. We instead instantiate a DR.JIT Loop object along with a pseudorandom number generator (PCG32), a counter (`i`), and a variable representing the final result.

```
from drjit.cuda import Loop, PCG32
rng = PCG32(size=1024 * 1024)
i, result = UInt32(0), Float(0)
loop = Loop(state=lambda: (rng, i, result))
while loop(si.is_valid() & (i < 128)):
    # ... loop body ...
    i += 1
```

This loop runs for only *one* iteration (the condition `loop(...)` returns **False** in the second round). This suffices to capture the effects of an individual loop iteration, which is all that is needed to wire² it into the generated kernel. A downside of our approach for embedding tracing into a host language is that DR.JIT must know about

²This involves the insertion of basic block boundaries and Phi nodes into the generated IR, which is in single static-assignment (SSA) form.

the loop’s *state variables*, which refers to variables that are modified in the body and either accessed in subsequent iteration or following termination. They are specified using a lambda function, which our implementation invokes before and after the loop to catch redefinitions of Python variables. The trace now looks as follows (rng seeding omitted for simplicity).



The specific loop of our example samples the cosine-weighted hemisphere and traces shadow rays.

```
while loop(si.is_valid() & (i < 128)):
    # Sample from cosine-weighted hemisphere
    sin_phi, cos_phi = dr.sincos(rng.next_float() * dr.TwoPi)
    sin_theta_2 = rng.next_float()
    wo_local = Vector3f(cos_phi * dr.sqrt(sin_theta_2),
                        sin_phi * dr.sqrt(sin_theta_2),
                        dr.sqrt(1 - sin_theta_2))
    # Rotate sample into shading frame and spawn ray with length 1
    ray_2 = si.spawn_ray(si.sh_frame.to_world(wo_local))
    ray_2.maxt = 1
    # Compute the number of unoccluded and increase iteration count
    result[~scene.ray_test(ray_2)] += 1.0
    i += 1
```

Finally, we reshape the 1D `result` array into a 2D image and write it to disk. It is at this point that the actual computation takes place within a generated megakernel containing all steps of this example (except for the variable `x` that was separately evaluated).

```
from drjit.cuda import TensorXf # Arbitrary-rank float32 tensor
from Mitsuba.core import Bitmap
tensor = TensorXf(result/128, shape=(1024, 1024)) # Reshape/scale
Bitmap(tensor).write('out.exr')
```



3.1 Discussion

Following this introductory example, we are in a better position to contrast DRJIT to other systems and review its constraints and goals.

Why not use standard array programming tools (PyTorch, JAX, TensorFlow) for this? Indeed, some of them provide operations resembling steps of the previous example. For example JAX [Bradbury et al. 2018] provides the `jax.lax.fori_loop()` and `jax.lax.switch()` operations to trace loops and dynamically dispatch to a set of Python functions, preserving the control flow for subsequent compilation by XLA [Google 2017]. We initially implemented a small renderer using these primitives, but found that compilation timed out on nontrivial examples. Figure 4 attempts to get to the bottom of this using a series of micro-benchmarks.

When unrolling loops, we observe significantly increased backend compilation time in JAX. While tracing via `jax.lax.fori_loop()`

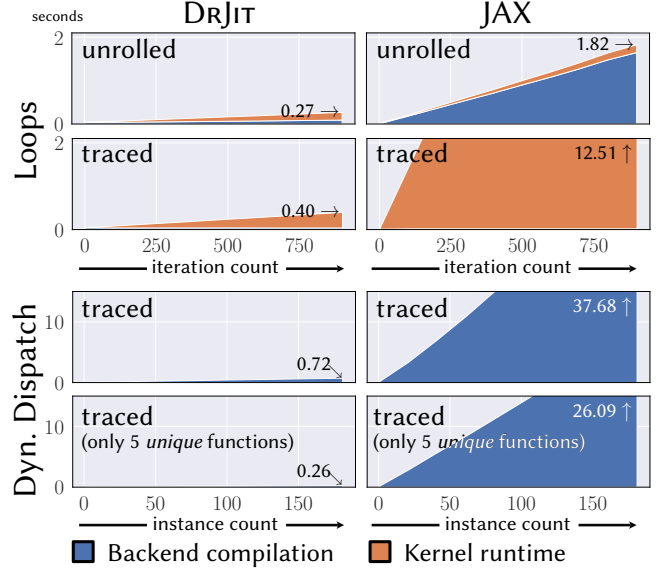


Fig. 4. Micro-benchmark comparing the tracing features of DRJIT and JAX. The top half benchmarks a simple loop with an update of the form $x = (x+1) \wedge x$ (x is a 1D array of 10^9 32-bit integers) with loop counts increasing from 1 to 1000 on the horizontal axis and combined compilation and runtime in seconds on the vertical axis. The bottom half benchmarks dynamic dispatch to an increasingly large set of functions f_1, f_2, \dots implementing successively better approximations of the sine power series, i.e., $f_i = \sum_{k=0}^i -1^k / (2k+1)! x^{2k+1}$. In the last row, the functions f_i internally take i modulo 5, which means that there are only 5 unique functions. This in principle provides an opportunity to greatly reduce the size of the program.

addresses this, the generated code curiously commits all loop state to memory at every iteration, which increases runtime cost. As its name indicates, `jax.lax.switch()` produces a `switch { }`-like statement that effectively merges all functions into the body of the generated kernel. This produces a very large IR representation that exacerbates the cost of steps like register allocation. DRJIT generates indirect calls to subroutines that admit separate compilation.

In the context of rendering, dynamic dispatch often targets functions that later turn out to be identical, which DRJIT exploits to reduce backend compilation time to a constant. XLA detects and exploits these redundancies, albeit with a runtime cost that grows with the size of the input program. The general pattern that emerges from these experiments is that the richness of ML-centric IR and optimizations passes (contraction of tensor operations, fusion, etc.) come at a significant extra cost.

Objectives. DRJIT is principally a framework for tracing large amounts of embarrassingly parallel computation; tracing constitutes its only mode of operation and takes place all the time. Our experimental evaluations routinely create and tear down between hundreds of thousands to multiple millions of variables for an individual rendering or differentiation step, and these operations are consequently highly tuned.

A key goal is that the entire process of Monte Carlo rendering can be captured without intermediate evaluation, returning the image in the form of a trace describing the computation needed to produce it.

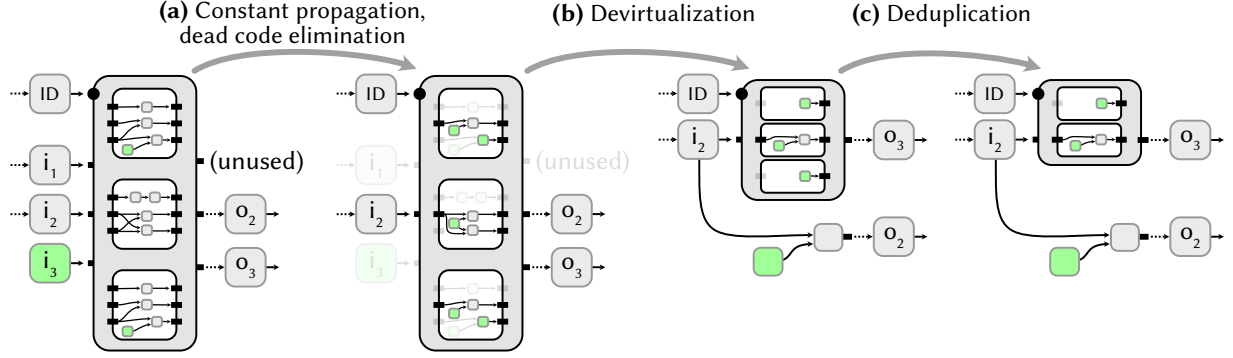


Fig. 5. When DR.JIT encounters a polymorphic method call, it traces the implementation of all reachable instances and performs multiple optimizations. In the example shown above, a call with inputs (i_1, i_2, i_3) returns outputs (o_1, o_2, o_3) . The variable i_3 is a constant literal, and the surrounding program only references outputs o_2 and o_3 . (a). DR.JIT propagates the constant into the captured sub-traces, while at the same time eliminating dead code across the call boundary. (b). In this example, all sub-traces perform the same computation to produce o_2 , and the computation is subsequently *devirtualized*, i.e., moved out of the call. (c). Finally, two of the sub-traces are found to be identical and only produce a single function definition during kernel assembly.

Loops and polymorphism must be preserved in this trace; the latter should be transformed into subroutines that admit separate compilation to avoid the creation of an immensely large program that breaks the backend compiler.

We now focus our attention on an important set of transformations that take place during and after tracing to substantially improve the efficiency of the generated code.

3.2 Optimizations

The need to optimize within DR.JIT may at first appear counter-intuitive, as backend compilation of the generated kernel IR via LLVM or OptiX/CUDA will subject it to dozens of sophisticated optimization passes. It appears that any simplifications made at this stage would simply be subsumed by later steps. While this intuition generally holds, it does not apply to dynamic dispatch that presents an opaque boundary impeding further optimization in these tools.

To connect with the previous example, recall the large data structure detailing the differential geometry of the primary intersection, of which only the position and shading coordinate frame were ultimately used. Since we are already JIT-compiling, why not generate a special version of the call that omits unreferenced outputs including the computation needed to produce them?

This train of thought leads to a set of global optimizations illustrated in Figure 5: first, we propagate constant literals into the call, where it may trigger simplifications (this is especially effective in differentiated programs, which tend to propagate many zero-valued derivatives). Removing unreferenced outputs removes unreferenced inputs, which may further cascade into the surrounding program. We also devirtualize computation that is identical in all sub-traces.

All of these optimizations are easily performed while tracing: constant propagation happens automatically, dead code elimination directly follows from variable reference counting, and deduplication leverages the value numbering optimization: if all sub-traces output a variable with the same ID, it can be moved out of the call.

Finally, identical traces will collapse into a single subroutine declaration during compilation. This optimization is essential for

rendering, where the scene definition may instantiate thousands of objects of the same type that may ultimately generate the same sub-traces. We note that this type of redundancy should be detected and exploited but cannot be assumed to hold in general: for example, an *ubershader*-type material like Disney’s Principled BSDF [Burley 2015, 2012] may expand into opaque or thin versions with 10-11 texturable parameters each, of which a different subset is active in each instance. Textures could be procedural, driven by 2D bitmaps or 3D volumes (potentially with different wrapping or filtering modes), based on mesh attributes, and in spectral variants of the system this could furthermore involve spectral upsampling or custom spectral profiles. When differentiation is later added on top, a subset of these parameters may require derivative tracking to solve an optimization problem. In essence, we cannot know what code a particular instance will produce; the only way to find out is to trace its evaluation and sampling procedures and examine the output of this process.

3.3 Dynamic dispatch to closures

One subtle but important detail that was omitted so far is the handling of instance attributes. As a motivating example, suppose that we implemented a textured Phong-style BRDF from scratch (ignoring subtleties like texture filtering and energy conservation):

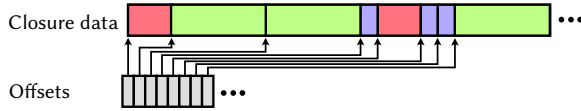
```
class Phong(mitsuba.render.BSDF):
    def __init__(self, albedo: TensorXf, exponent: Float):
        self.albedo = albedo # Bitmap data (TensorXf)
        self.exponent = exponent # Specularity (scalar Float)

    def eval(self, si: SurfaceInteraction3f, wo: Vector3f):
        # Convert UV into texel coordinates and perform a lookup
        resolution = Vector2u(self.albedo.shape)
        pos = dr.min(Vector2u(si.uv * resolution), resolution - 1)
        albedo = self.albedo[pos.y, pos.x]
        # Evaluate reflected direction and BRDF terms
        r = Vector3f(-si.wi.x, -si.wi.y, si.wi.z)
        return albedo * dr.InvPi + dr.dot(r, wo) ** self.exponent
```

Evaluation accesses two attributes: `albedo`, which refers to a region in device memory, and a scalar `exponent` controlling specularity.

Both are implicit variable dependences that must somehow be represented in the generated kernel. While DR.JIT could paste the actual pointer and exponent values into a generated IR, doing so would interfere with the previously mentioned optimizations, causing non-identical Phong instances to compile into distinct subroutines.

The problem here is that instead of merely tracing functions, the system also needs to handle *closures*, which refers to pairings of functions with data from a surrounding environment. Tracing and kernel assembly should then separate code from data so that optimizations remain effective. DR.JIT transparently performs this optimization by detecting implicit variable dependencies while tracing reachable implementations of a polymorphic function call. Their contents are written into a contiguous array along with an auxiliary offset array that indicates the closure data referenced by specific instances.



The creation of these arrays proceeds asynchronously by a builtin kernel that collects implicit dependencies from various locations in device memory. The total amount of device memory needed for them is small—usually on the order of a 10-100 KiB per method call³.

3.4 Additional features

Vectorization. The LLVM backend of DR.JIT generates vectorized IR according to the SIMD instruction set present on the host machine. In practice, this means that all operations including loops, dynamic dispatch, and ray tracing process 4-16 elements at a time, which requires additional masking that DR.JIT introduces automatically. Function calls generally require several iterations to process all elements in the presence of divergence. These steps are reminiscent of ISPC [Pharr and Mark 2012] that performs similar transformations. Closure conversion and deduplication of identical functions in DR.JIT are important steps in reducing divergence during vectorized execution on the CPU and GPU.

Side effects. Several of DR.JIT’s builtin operations like scatter operations and atomic scatter-reductions mutate existing arrays. Read access or arithmetic involving variables marked as being affected by queued side effects trigger a kernel launch to materialize them. This simple greedy schedule works well for our applications, though we note that array programming compilers like XLA can potentially find a more optimal decomposition into kernels using global analysis of the computation graph.

Loop optimizations. Besides polymorphism-related optimizations, DR.JIT also optimizes loop constructs by removing state variables that are unreferenced or invariant. Again, these steps would normally be subsumed by optimization passes in LLVM or OptiX. However, given DR.JIT’s global view through arbitrary sequences of polymorphic method calls, recursion, and loops, it is in a better position to infer such redundancies.

³Large device arrays like textures or volumes are accessed *indirectly*. The closure data array records a pointer to them rather than the data itself, while scalars are directly copied to reduce an unnecessary indirection.

Wavefront-style evaluation. DR.JIT exposes a set of flags to control fundamental aspects of tracing. They can be used to disable special handling of loops and dynamic dispatch, causing them to be “unrolled” analogous to the wavefront evaluation performed by the Enoki library [Jakob 2019]. In the case of dynamic dispatch, the system groups the wavefront by instance, launching a kernel per group.

3.5 Results

We now turn to a first set of results that examine the performance of DR.JIT on *primal* rendering workloads, comparing it to two open source renderers with wavefront-style evaluation: PBRT (version 4) [Pharr et al. 2020] and an unmodified version of Mitsuba 2 [Nimier-David et al. 2019] running on top of the Enoki [Jakob 2019] library.

Experiments throughout this article were performed on an AMD Ryzen Threadripper 3990X Linux server (64+64 virtualized cores, 128 GiB of RAM) with an NVIDIA RTX A6000 graphics card (45.6 GiB of RAM) for hardware-accelerated ray tracing via OptiX. The thermal design power (according to vendor specification) of CPU (280W) and GPU (300W) are roughly matched to also enable a fair comparison between these two very different processor architectures. On the CPU, we followed best practices for benchmarking like disabling security mitigations for side-channel attacks and pre-allocating *huge* pages (2MiB) as recommended by Embree [Wald et al. 2014].

The benchmark scenes are shown in Figure 8 and represent varied application scenarios: the *staircase* scene is composed of 749 shapes and 24 BSDFs, requiring efficient handling of polymorphism. We render it with relatively low-order scattering, while using a larger path depth of 12 interactions in the *Living room* scene. The *Glass of water* simulation accounts for up to 32 successive refractions and reflections in a scene with many dielectric boundaries, though only a subset of paths requires this many interactions.

Three groups of columns in Figure 6 contrast classic one-ray-at-a-time rendering with static C++ compilation (“scalar”), execution via LLVM, and OptiX. DR.JIT results are presented in both wavefront and megakernel mode. Our system compiles a specific megakernel (or series of smaller kernels) for each scene, which incurs a one-time overhead that is represented by hatched bars; the solid portion below indicates performance once the system is warmed up. While incorporating DR.JIT into Mitsuba 2, we applied minor optimizations to the base renderer, such as marking primary rays as coherent in Embree. These also benefit the renderer’s scalar mode (which technically involves no JIT compilation), which we represent by the green DR.JIT bar in the “Scalar (CPU)” column.

Overall, performance compares favorably to existing tools, achieving geometric mean speedups of 2.66× (Mitsuba) and 1.64× (PBRT) on the GPU. LLVM megakernels produced by our system are often surprisingly competitive with the GPU backend.

Compilation into wavefronts produces programs that must repeatedly read and write vast amounts of data, imposing a burden on the processor’s memory subsystem. Difference in memory bandwidth on the CPU (95.37 GiB/s) and GPU (715 GiB/s) as well as latency hiding-capabilities in the latter lead to marked differences between architectures in this case. Wavefront-style execution reduces GPU performance by a factor of 1.3 – 7.5×, while the same experiment on the CPU can increase cost by a factor of more than 100×.

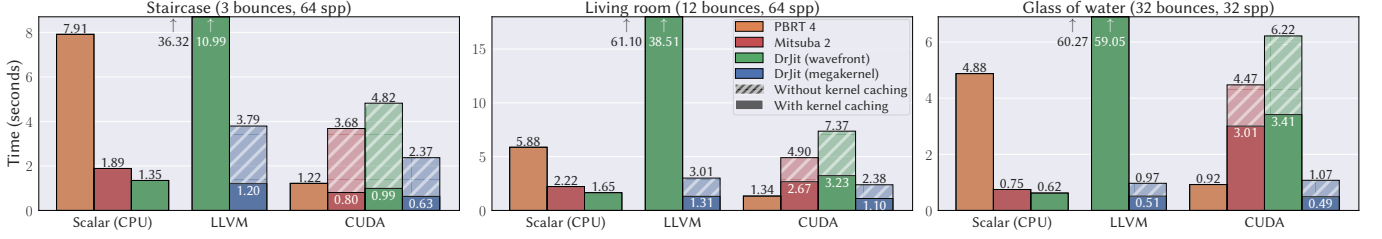


Fig. 6. We compare the performance of Dr.Jit to PBRT (version 4) [Pharr et al. 2020] and an unmodified version of Mitsuba 2 [Nimier-David et al. 2019], rendering three scenes of varied complexity that are shown in Figure 8. Both megakernel and wavefront-style evaluation are shown for Dr.Jit, where hatched bars indicate the one-time backend compilation cost (the actual kernel runtimes are listed just below). PBRT is statically compiled and do not have this overhead. The performance figures demonstrate that OptiX and LLVM megakernels produced by Dr.Jit achieve state-of-the-art performance.

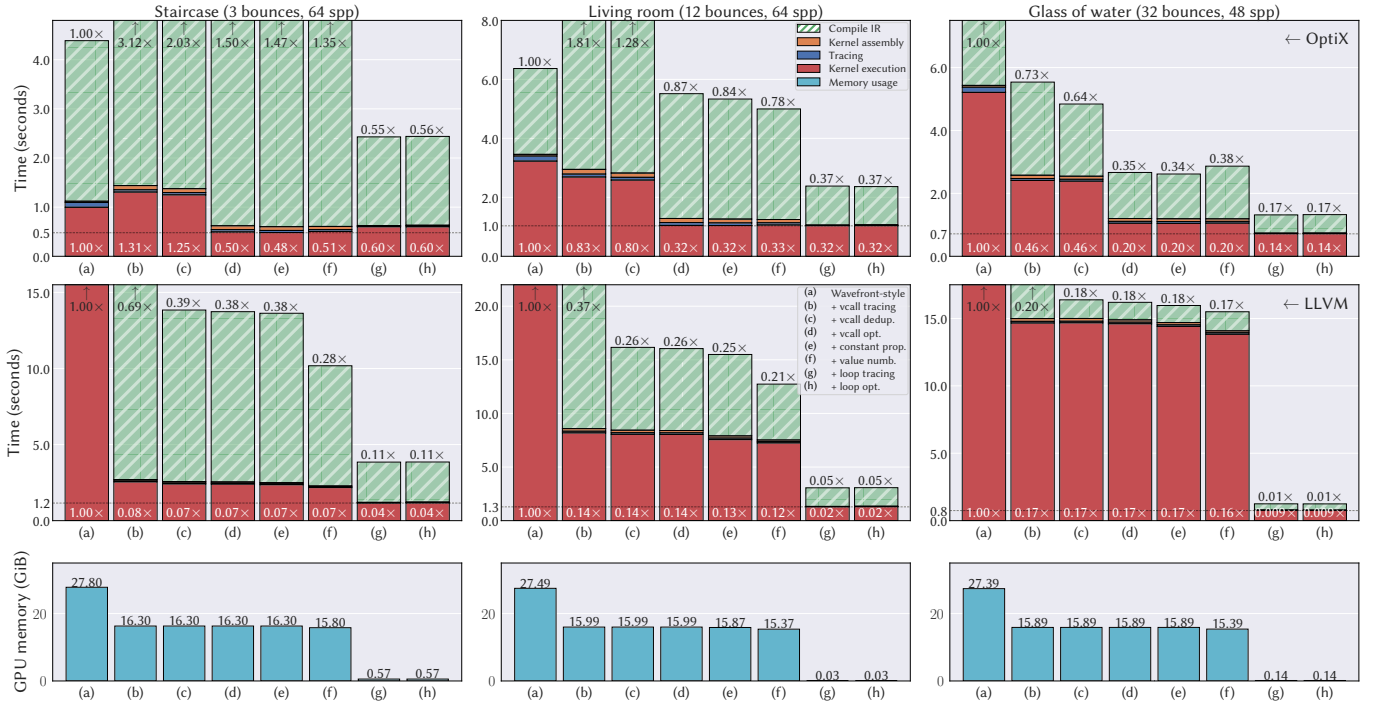


Fig. 7. Using the same set of scenes, we investigate the effect of different optimizations in Dr.Jit. The three rows depict OptiX and LLVM runtime costs followed by peak memory usage that is identical in both backends. Stacked bars indicate the time spent on backend IR compilation (hatched), kernel assembly (orange) and tracing (blue) within Dr.Jit, as well as kernel execution (red). The leftmost bar (a) is a wavefront baseline that “unrolls” all use of loops and polymorphism into separate kernels that communicate through global memory. Going from left to right, we then successively enable (b) compilation of polymorphism into subroutines, (c) deduplication of subroutines containing identical code, (d) global polymorphism-aware optimizations (Section 3.2), (e) constant propagation, (f) local value numbering, (g) tracing loops instead of unrolling them, and (h) loop state optimizations.

Figure 7 investigates the effect of individual optimizations starting from a wavefront-style baseline resembling the operation of the Enoki library (column a). Memory usage is significant in this configuration (bottom row). Although peak usage could be reduced by launching many smaller wavefronts, it does not address the fundamental issue that a large amount of data will need to be read and written many times.

A high level observation is that tracing and kernel assembly (orange and blue bar regions) only constitute a small portion of the total computation time. The precise amount tends to be lower when compiling megakernels and higher for wavefronts requiring multiple

rounds of tracing and assembly. Backend compilation time to transform IR into machine code can be significant (longer than the kernel execution itself), which can make the system unsuitable for certain use cases and emphasizes the importance of caching mechanisms.

Mapping polymorphic function calls to subroutines in (b) drastically reduces runtime on the CPU while increasing compilation time on both backends; subroutine deduplication in (c) reverts most of the growth in compilation time and also gives a speed boost thanks to reduced divergence under vectorized execution.

Removing unreferenced computation, arguments, and return values from polymorphic method calls in (d) has a surprisingly large

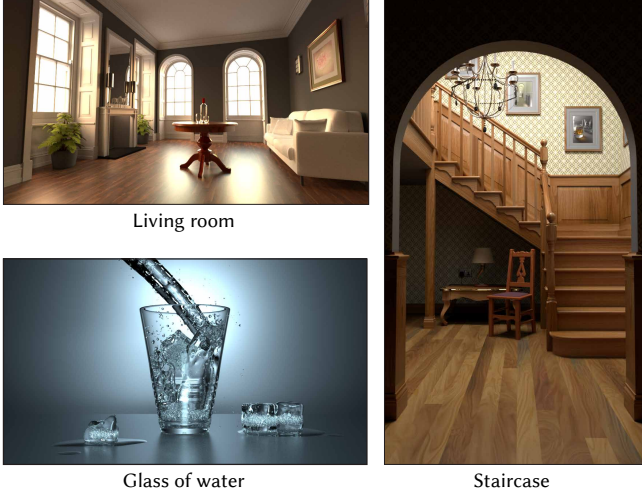


Fig. 8. Scenes from Bitterli’s [2016] rendering resources used in benchmarks.

effect in the OptiX backend, where it generally improves performance by a factor of 2×, while having essentially no impact on the CPU. Modern superscalar CPUs can absorb a certain amount of redundant computation by issuing multiple instructions per clock cycle. We speculate that these architectural features along with the lower cost of data exchange through the stack could be responsible for the modest benefit of this optimization (though it will prove to be more effective when applied to differential kernels in Section 4).

Loop tracing reduces memory traffic to an absolute minimum, which greatly benefits CPU execution, while the effect on the GPU is inconclusive. We speculate that loops may exacerbate the OptiX conversion into a state machine, whose nodes must exchange continuation state [Parker et al. 2010]. Loop optimizations remove many state variables (details in Section 4.11), but this does not have a measurable effect on runtime performance. We suspect that they are subsumed by backend optimization passes in this case.

3.6 Limitations

Before continuing to the derivative case, we discuss notable limitations of the tracing approach.

Debugging. Remote-debugging GPU kernels on a CPU bridges two asynchronously operating computing devices and is generally known to be difficult. The addition of tracing adds yet another level of asynchronicity, exacerbating these challenges. We provide two basic ways to investigate the behavior of a program: when set to full wavefront-style evaluation (Section 3.4) the user can set breakpoints, step through the program, and investigate variable contents. When compiling to megakernels, this approach, however, conflicts with the central tenet (“do not split the megakernel”). Our only current option is to insert debugging statements (`dr.printf_async()`) that will print from the device at some later point when the kernel executes. Future work will be needed to develop more refined debugging primitives for this unusual way of performing computation.

The need to evaluate. Some aspects of our system can be non-intuitive to new users. For example, suppose we wanted to run the ambient occlusion integrator multiple times to produce a sequence

of uncorrelated Monte Carlo estimates. This is easily accomplished via continued use of the defined pseudorandom number generator `rng`. However, the user would then find that kernel caching is ineffective (every iteration launches a costly backend compilation step), and these kernels furthermore become bigger and slower over time. This happens because we never asked the system to materialize the RNG state; all of the RNG state updates from prior rendering steps spill over into the current kernel, which steadily grows as a consequence. A simple `dr.eval(result, rng)` statement resolves this but requires a certain degree of awareness of how tracing works.

Scope. As mentioned earlier, DR.JIT is not a general-purpose array programming language. While two previous code fragments involved an n -d array abstraction named `TensorXf`, doing all computations in terms of tensors is discouraged. For example, slicing this tensor within rendering code might break the megakernel into parts to exchange information between different Monte Carlo samples. We provide tensorial types for interoperability with other machine learning tools, and to represent shaped data like images or volumes.

Recursion. DR.JIT can trace dynamic dispatch to functions that themselves perform dynamic dispatch, which is, e.g., needed to handle object transformations involving instanced geometry. Cycles including self-recursive calls are not permitted and lead to infinite recursion, as the system will trace the same code repeatedly without knowing when to stop. We believe that this could be detected and handled by reusing previously generated subroutines but have not implemented such a feature in our present system.

4 AUTOMATIC DIFFERENTIATION

Following this presentation of DR.JIT’s computational foundation, we can now turn to its facilities for automatic differentiation. To motivate this part of the system, we will discuss the high-level architecture of recent differentiable rendering techniques and the constraints that they pose on the evaluation of derivatives.

Differentiation transforms how something must be computed, and in the context of rendering it inflates the size and complexity of a primal algorithm. There are several reasons for this: first, reverse mode runs into the discussed issue (Section 2) that vast amounts of intermediate program state must later be recalled, which can be avoided by recomputing intermediate results using physical reciprocity and mathematical invertibility. Second, rendering algorithms integrate discontinuous functions, which produces *bias* when naïvely differentiated (e.g., via direct application of AD); extra steps must be inserted into the derivative to avoid this. Finally, differentiation must in general evaluate a differential version of every continuous variable in the program, which further increases its size⁴.

Differentiation in DR.JIT occurs at a higher architectural level but depends on the JIT compiler as foundation. Their combination exploits the unusually dynamic nature of differentiation: depending on the optimization task specified by the user, derivatives are only needed in a small subset of program variables. Using dynamic code generation and a global view of what can ultimately affect the computed result, we are able to quickly produce differential algorithms that adapt to the scene and problem statement.

⁴This size-increase is problem-dependent, though values of 3 – 5× are representative.

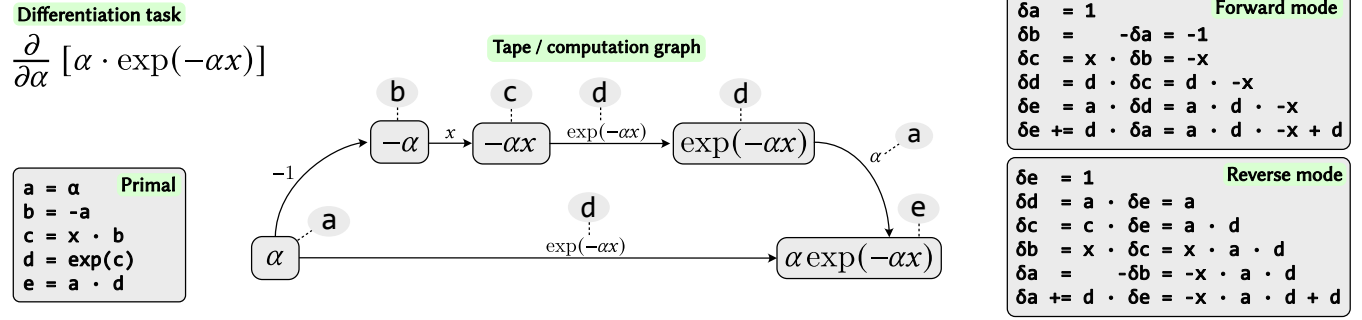


Fig. 9. An example use of tape-based forward/reverse-mode AD to differentiate the exponential density $\alpha \exp(-\alpha x)$ with respect to α . The variable x does not carry derivatives (it is *detached*) and could, e.g., represent a Monte Carlo sample position. Primal evaluation of this expression (bottom left) generates a sequence of temporaries (a, b, c, d, and e) and replicates the dependency structure of their computation in a tape/computation graph (middle). Each edge in this graph carries a weight indicating the sensitivity of the target node with respect to perturbations of the source node. Often, these edge weights are simply variables of the primal program, which is indicated by ellipses. AD associates a derivative variable with each temporary and program variable (e.g., a and δa). Forward- and reverse modes (right) traverse the tape as indicated by their name, propagating derivatives scaled according to the edge weights. The result is equivalent, though the efficiency of the two modes can drastically differ when the computation has many inputs or outputs.

4.1 Tracing and the directionality of differentiation

The discussion of related work (Section 2) outlined two high-level flavors of AD: *tracing*, and *source transformation*. At the outset, DR.JIT uses what appears to be a standard tracing approach, which means that it records the structure of the computation and its dependence on differentiable inputs at runtime. However, combined with dynamic compilation and function-level differentiation of polymorphic constructs, it becomes a hybrid that lies in between these extremes.

Before reviewing AD fundamentals and explaining our approach, we note that future use of the word *tracing* now takes on a different meaning and refers to a (*Wengert*) *tape*, or *computation graph* that captures operations for subsequent derivative propagation. This occurs one architectural level above JIT tracing explained in Section 3; the combined system therefore traces at *two* levels simultaneously.

Figure 9 provide an illustrative example of AD tracing: the system captures every differentiable operation on a tape, whose later traversal computes a differential version δx of every program variable and temporary x . This process can either take place in forward or reverse mode, which are suitable for different kinds of problems (Section 2).

When f is a rendering algorithm, forward mode computes the derivative of the rendered image (Figure 1) with respect to a single parameter or a linear combination of multiple parameters. Many separate passes are needed to differentiate all scene parameters (typically in the millions), making forward mode unsuitable⁵ for optimization. However, the development of Monte Carlo renderers sometimes requires investigating images contaminated by noise or bias to identify potential causes, and we find that intuition about such deficiencies partially extends to forward mode derivative images. DR.JIT supports forward differentiation mainly to enable this type of debugging workflow. Typical applications of differentiable rendering optimize nonlinear objectives on spaces with large numbers of unknowns, which requires reverse mode.

⁵When derivative images are truly desired, it is important to note that reparameterizations or edge sampling for unbiased visibility handling add considerable runtime cost. Consequently, it is normally more efficient to obtain them via finite differences and multiple primal renderings with correlated random number streams to reduce variance.

When contrasting primal and reverse-mode rendering, we observe that the former is mostly a *read-only* process, in which a set of stochastically generated rays samples the scene representation. The reverse-mode derivative of a read in a computer program produces a *write*, which turns the derivative of the rendering algorithm into a *write-heavy* method that accumulates gradients into every scene parameter encountered by a light path.

4.2 Objectives

A central tenet of Sections 1 and 3 was that the system should never unnecessarily break a Monte Carlo rendering step into multiple pieces, which required preserving control flow constructs like loops and polymorphic function calls during tracing.

This objective remains essentially unchanged and also influences our approach to differentiation. To generate an efficient *differential megakernel*, we need to map primal computation onto its derivative while preserving these traits. The system must, e.g., turn closure calls into calls to forward- or reverse-mode derivatives of closures. Their implicit dependence on scene parameters complicates this process and will require special treatment.

Loops are a frustrating element of AD in both tracing and source transformation approaches due to their unpredictable storage requirements (Section 2.1). Our perspective on them is that the automatic derivative of a loop is almost never satisfactory, and that the developer should instead contribute domain-specific knowledge to provide an equivalent *custom adjoint*. Our system provides this capability and does not attempt to differentiate traced loops⁶.

4.3 Tracing with dynamic compilation

DR.JIT’s interface to automatic differentiation follows the conventions of standard array programming tools. For example, the

⁶We retain the ability to differentiate unrolled (wavefront-style) loops with checkpointing, which is useful to validate such custom adjoints or differentiate rendering algorithms that have not been specifically modified to support differentiation.

exponential density derivative from Figure 9 would be expressed as

<pre>x, α = ... dr.enable_grad(α) e = α * dr.exp(-α * x) dr.backward(e) δa = dr.grad(α)</pre>	<pre>x, α = ... dr.enable_grad(α) e = α * dr.exp(-α * x) dr.forward(α) δe = dr.grad(e)</pre>
--	---

Traversal of the tape produces a flurry of operations referencing primal program variables (α , x , e), which is illustrated on the right of Figure 9. A subtle but important point is that these operations involve *traced* variables provided by the underlying JIT compiler.

By default, operations like `dr.forward()` and `dr.backward()` de-struct the AD graph while traversing it, *materializing* the steps that are necessary to compute the desired derivatives. Or said overly dramatically, the AD data structures self-destruct, leaving a residue of ordinary computation. This residue is traced by the JIT-compiler one level below so that it can run as part of a (mega-) kernel at some later point. The actual destruction of the AD graph turns out to be immaterial in this process; it is often useful to retain it when multiple AD traversal steps are needed. This idea is not a contribution of DR.JIT and also underlies other hybrid AD techniques combining tracing with code generation, e.g., CppADCodeGen [Leal and Bell 2017].

Another observation is that this combined system supports *checkpointing* without having put any intentional effort into realizing such a feature. Consider an unrolled loop with intermediate evaluation:

```
for i in range(1000):
    data = f(data) # 'f' represents a potentially complex
    dr.eval(data) # transformation of 'data'.
    dr.backward(data) # Now, backpropagate through all steps
```

The AD layer will reference intermediate steps and temporaries produced by the function `f` to enable subsequent differentiation, and these must be recomputed. The JIT layer knows how to compute these needed variables, and it will do so *from the last evaluation point* that therefore takes the role of a checkpoint. Checkpointing is not ideal for PBDR workloads due to the size of even a small number of checkpoints, though it does help when differentiating rendering techniques that have not been adapted for efficient differentiation.

4.4 Customizing differentiation

Like many other AD systems, ours also provides a mechanism to override or extend derivative evaluation (a *custom adjoint* in reverse mode terminology). Subclasses of `dr.CustomOp` provide primal-, forward-, and reverse-mode callbacks. The latter two are called when derivatives must be propagated across use of the `CustomOp` on the tape. A basic example is shown for a one-argument identity.

```
class MyOp(dr.CustomOp):
    def eval(self, value):
        return value
    def forward(self):
        self.set_grad_out(self.grad_in('value'))
    def backward(self):
        self.set_grad_in('value', self.grad_out())
result = dr.custom(MyOp, value) # Use 'MyOp' in a program
```

A nonstandard aspect of DR.JIT’s realization of this feature is the ability to track *implicit* inputs or outputs, i.e., dependencies that are not inherent from the function signature. When `MyOp` reads

and writes variables that are *not* function inputs or return values, its `MyOp.eval()` callback can register them retrospectively using `CustomOp.add_input/output(...)`. This ensures that the global flow of derivatives is correctly represented in the computation graph.

4.5 Differentiating polymorphism

With this infrastructure in place, we are ready to discuss polymorphism. We will consider the following method call, where `obj` refers to a DR.JIT array of instances that implement the function `func`.

```
out = obj.func(arg_1, arg_2, ..)
```

The derivative of such a polymorphic method call, is *another* polymorphic method call to JVP and VJP (Section 2.1) versions of the original set of functions. DR.JIT generates these dynamically as needed. To detect this need, it wraps use of polymorphism like the example above into a dynamically generated `dr.CustomOp`. Suppose that the `CustomOp.backward()` callback is now invoked during an AD traversal, which indicates that the system needs to propagate `dr.grad(out)` to `dr.grad(arg_1)`, `dr.grad(arg_2)`, etc.

To accomplish this, the AD layer dynamically defines a VJP version of each method implementation, which is simply a placeholder that calls `func` a second time, with recursive usage of AD to propagate and extract derivatives.

```
def func_vjp(grad_out, arg_1, arg_2, ..):
    dr.enable_grad(arg_1, arg_2, ..)
    result = func(arg_1, arg_2, ..)
    dr.set_grad(result, grad_out)
    dr.backward(result)
    return dr.grad(arg_1), dr.grad(arg_2), ..
```

The AD layer then issues a polymorphic method call to these newly defined functions. To realize this method call, the JIT layer traces each possible target, which runs all VJP placeholder functions, materializing the differentiation into ordinary computation.

Automatic discovery of implicit dependences. Section 3.3 observed that the functions being differentiated are generally *closures* that implicitly depend on further variables from a surrounding environment (e.g., instance attributes). In the context of rendering, a typical example would be a procedural texture or BSDF with model parameters influencing their appearance.

Such model parameters are neither inputs nor outputs; they create an implicit differentiable dependence that must be discovered and tracked by the AD system. Our system does this automatically by monitoring variable accesses during initial execution of the primal `CustomOp.eval()` callback, registering them using the previously discussed mechanism. The VJP (reverse mode) implementation of a method call with such implicit reads will issue atomic scatter-reductions to update scene parameters gradients. This is not just an odd corner case; it constitutes the main way in which scene parameter gradients are generated.

4.6 Review of PBDR algorithms and relevant properties

The combination of AD with dynamic code generation provides a useful foundation but does not indicate a clear path towards the goal we set out to accomplish: to compile the derivative of a rendering algorithm into a *differential megakernel*. Two more stumbling

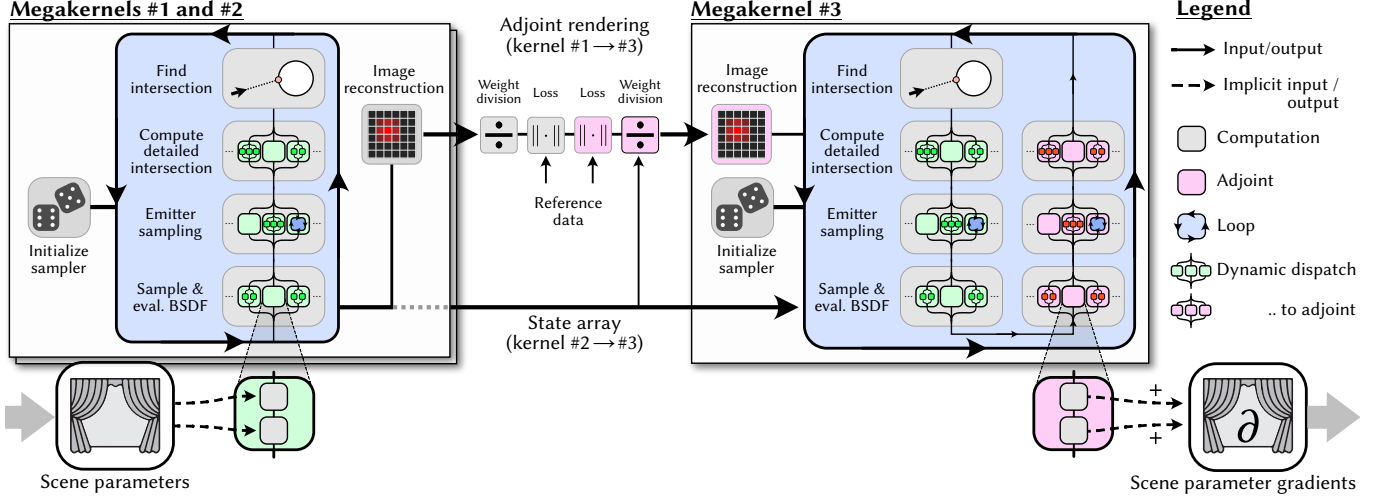
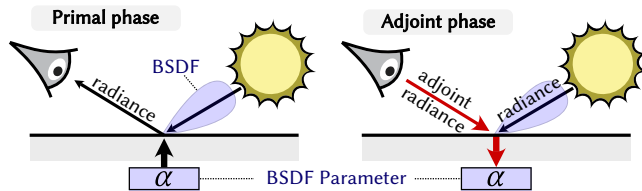


Fig. 10. The anatomy of a recent physically based differentiable rendering method. This diagram illustrates a partition of the major components of *Path Replay Backpropagation* (PRB) [Vicini et al. 2021] into a set of three self-contained megakernels that each solve a Monte Carlo integration problem. Megakernel #1 is a standard path tracer, which reads scene parameters to produce a *primal* rendering, using an image reconstruction filter to scatter weighted samples values into an output buffer with subsequent weight division [Pharr et al. 2020]. This is more costly than rendering with a *box* filter but ensures the differentiability of the full image formation process. A loss function then quantifies the quality of the current solution. Meanwhile, a second path tracing megakernel performs the same computation once more with a different pseudorandom seed and provides a per-sample state array to a final *adjoint* megakernel #3 (see Section 4.6 for details). This kernel contains adjoint versions of all steps (intersection, emitter sampling, and BSDF evaluation) that accumulate scene parameter gradients.

blocks must be navigated: how to deal with loops, and how partition derivative propagation into parts that *must* and parts that *must not* be handled within a megakernel. We will first review recent PBDR Methods and then cover these issues in turn.

Primal rendering algorithms like path tracing [Kajiya 1986] propagate *radiance* from light sources to the sensor. To do so, they generate consecutive path vertices in reverse order (i.e., starting at the sensor), which is normally done using loops. The significant amount of intermediate state that these loops can produce complicates the evaluation of reverse-mode derivatives.

Radiative Backpropagation (RB) [Nimier-David et al. 2020] addresses this challenge by reinterpreting the derivative of the simulation as an independent simulation propagating a differential quantity termed *adjoint radiance*. The adjoint radiance is easily computed in image space: it is the derivative of the image loss that, e.g., captures which pixels of the rendered image should become brighter or darker to reduce the loss function. Like a video projector, the camera then radiates this adjoint quantity into the scene, where it scatters just like normal radiance.



Whenever this adjoint radiance encounters a surface with differentiable parameters, it accumulates a contribution into the local parameter gradient vector, for example to optimize α above.

One issue with RB is that the accumulation must query the primal incident radiance as illustrated previously, whose computation is costly and incurs quadratic runtime cost. *Path Replay Backpropagation* (PRB) [Vicini et al. 2021] addresses this issue by splitting the differential phase into two sub-phases. The first phase performs a normal random walk and outputs a per-sample state vector that is passed to the second (adjoint) phase. Using the invertibility of arithmetic performed by the path tracer, is then possible to recover the needed incident radiance at every vertex on the fly. Altogether, the computation then consists of three main steps: a first *decorrelated* [Gkioulekas et al. 2016] primal rendering step that renders an ordinary image, and the two sub-phases of PRB to propagate derivatives. An diagram illustrating the high-level architecture is shown in Figure 10. This is the most basic version of this method, i.e., *detached* and *non-reparameterized*—differentiating perfectly specular material interactions and unbiased visibility handling requires extra steps. The combination of RB and reparameterizations was first presented by Zeltner et al. [2021]. We refer these papers for details; it is mainly their high-level structure that is relevant here.

Supplemental material. This article’s supplement contains commented Python implementations of several differentiable rendering algorithms implemented using DR.JIT, including `prb_basic.py` (a simplified version of PRB without direct illumination), `prb.py` (standard PRB), and `prb_reparam.py` (reparameterized PRB). They provide a more complete view of differentiation-related challenges, and how such methods can be implemented on top of DR.JIT.

4.7 Isolation boundaries

At every scattering interaction, RB or PRB perform a differentiable computation and then backpropagate through its computation graph.

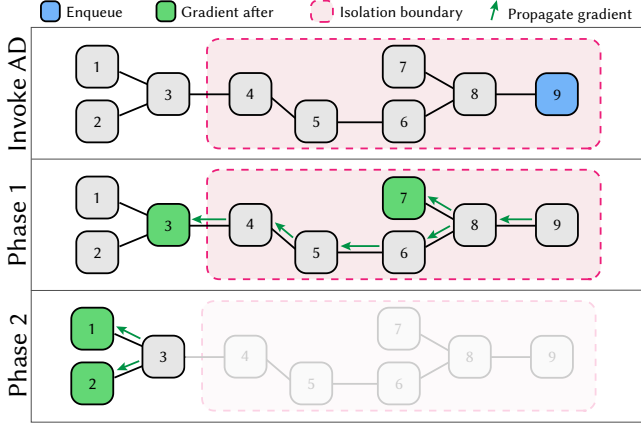


Fig. 11. DR.JIT provides three different AD scopes. The first is an *isolation boundary*. Wrapping computation into such a scope restrains the process of derivative propagation: only edges within and just across the isolation boundary may be traversed, while others are postponed until the scope is destroyed. DR.JIT uses this feature to ensure correct generation of a differential megakernel that is embedded within a larger differential calculation.

An exemplary fragment is shown below, where L_i , L_r and δL refer to incident, reflected, and adjoint radiance.

```
while loop(depth < max_depth):
    # ... Compute surface interaction 'si' ...
    Lr = Li * si.bsdf().eval(si, wo) # Reflected radiance from 'wo'
    dr.backward( $\delta L * L_r$ ) # Backpropagate product
```

Monte Carlo rendering is usually part of a larger calculation, which now leads to a complication: the AD traversal above is likely to encounter operations, whose differentiation would break the megakernel. For example, the BSDF could query a texture, whose MIP levels were previously computed using successive reductions. The derivative of this process must upsample gradients back to the finest level, requiring multiple passes with intermediate data exchange, which cannot be practically done at this stage. DR.JIT provides *isolation boundaries* (Figure 11) to *postpone* such problematic steps, enabling the generation of megakernels that still ensure correct global propagation of derivatives.

```
with dr.isolate_grad():
    # .. temporarily isolate outside world from AD traversals ..
```

Loops and polymorphic calls implicitly create an isolation boundary.

4.8 Parameterizations

Parameters influencing the position and shape of scene geometry produce bias when differentiated (Figure 12) unless the Monte Carlo integrals within the rendering algorithm are reparameterized. Reparameterizations have the purpose of counteracting parameter-dependent silhouette motion so that discontinuities are *frozen* when observed within spherical integrals. When building PBDR methods on top of DR.JIT, we prefer to expose reparameterization through a CustomOp-based abstraction to isolate their specifics from the surrounding computation. A differentiable re-parameterized ray intersection then reduces to two lines:

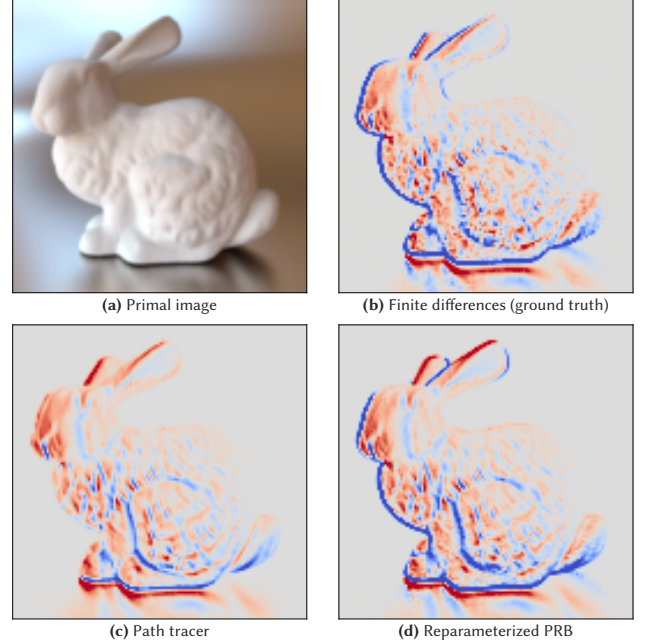


Fig. 12. Derivatives of parameters that affect the visibility in a scene are generally biased unless special precautions are taken. This figure illustrates the forward mode derivative of a translating Stanford bunny on a glossy metallic floor. (a) Primal rendering. (b) Reference. (c) Naïve differentiation of a path tracer. This result is severely biased, which manifests in missing silhouette gradients; their indirect reflection in the floor also shows marked discrepancies. (d) Reparameterizing all integrals resolves this problem.

```
ray.d, det = reparameterize(ray)
si = scene.ray_intersect(ray)
```

Here, \det is Jacobian determinant of the change of variables.

Reparameterizations are a somewhat strange concept. In ordinary (primal) computation, they reduce to an identity function—for example, the `eval()` callback of the custom operation simply returns the input ray direction along with a Jacobian determinant of 1.

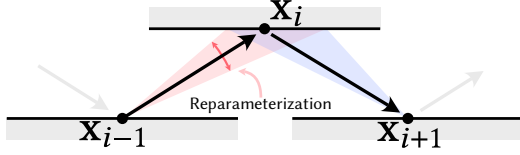
When differentiated, they expand into an intricate sequence of steps (Figure 13) that entail tracing auxiliary rays, weighting them, and using AD to scatter scene parameter gradients into intersected shapes. Usage of AD is therefore recursive in our system: A top-level `render()` function launches PRB (a CustomOp) when differentiated, which differentiates path contributions in a traced loop and thereby evaluates the derivatives of various system operations including parameterizations (a CustomOp), which launches differentiable ray tracing operations (a CustomOp). Another level of recursion may take place in the presence of instancing.

```
render(scene)
└─ Path Replay Backpropagation (CustomOp)
    └─ Reparameterization (CustomOp)
        └─ Shape.compute_surface_interaction (CustomOp)
```

4.9 Fine-grained derivative tracking

The differential integrators in the supplement contain loops with nested use of AD to compute light path derivatives *one vertex at a time*.

When reparameterizations are additionally used, this leads to difficulties, since they perturb the positions of these path vertices.



For example, a position perturbation of x_i changes the BSDF's value at the adjacent vertices x_{i-1} and x_{i+1} . Reparameterized integrators must reevaluate these BSDF terms with AD to ensure that these additional derivative terms are correctly computed. However, this now leads to the problem that the derivative of these terms will also produce derivatives with respect to *scene parameters* (e.g., the roughness at x_{i-1} and x_{i+1}), which is *not* wanted in this context. We only wish to differentiate the BSDF's dependence on the direction towards x_i .

To address these and similar issues, DR.JIT's AD layer keeps track of a set of variables Ω for which derivative tracking is currently enabled. Two additional *AD scopes* modify this set, by setting it to the empty set (\emptyset), its complement, or by adding and subtracting variables from the current set. The typical structure of a PBDR algorithm using these abstractions repeatedly enters and leaves scopes to carefully control what derivative terms should be generated.

```
with dr.suspend_grad():                #  $\Omega = \emptyset$ 
  with dr.resume_grad():                #  $\Omega = \emptyset^c$ 
    ray.d, det = reparameterize(ray)
    si = scene.ray_intersect(ray)
    # .. detached sampling steps ..
  with dr.resume_grad(ray.d):          #  $\Omega = \{\text{ray.d}\}$ 
    # Only account for directional derivatives at 'si_prev'
    L += Li_prev * si_prev.bsdf().eval(si_prev, ray.d)
    # .. other steps ..
  with dr.resume_grad():                #  $\Omega = \emptyset^c$ 
    dr.backward(∂L * L) # Backpropagate through all terms
```

An important detail is that CustomOp instances must capture the current scope at evaluation time so that it can be temporarily re-instated when running the associated forward- or reverse-mode callback. Combined with differentiation of polymorphic calls, this will then generate custom JVP/VJP variants of functions.

4.10 AD tape surgery

The supplemental PBDR code contains many steps of the form

```
Lr_diff = Lr * (bsdf_value_diff / bsdf_value)
```

where `bsdf_value` represents a side product of a *detached sampling strategy* (i.e., it is not considered during differentiation). This term is also a factor of another variable (e.g., `Lr`, the reflected radiance). To compute desired derivative terms in `Lr`, the program then divides out `bsdf_value` and multiplies by an *equivalent* `bsdf_value_diff` that is, however, computed *with* derivative tracking. Such steps can trigger significant extra computation besides the division, affecting primal and adjoint programs. We provide the `dr.replace_grad(a, b)` function that combines the primal value of 'a' with the AD trace of 'b' to avoid this behavior, which changes the previous example to

```
Lr_diff = Lr * dr.replace_grad(1, bsdf_value_diff / bsdf_value)
```

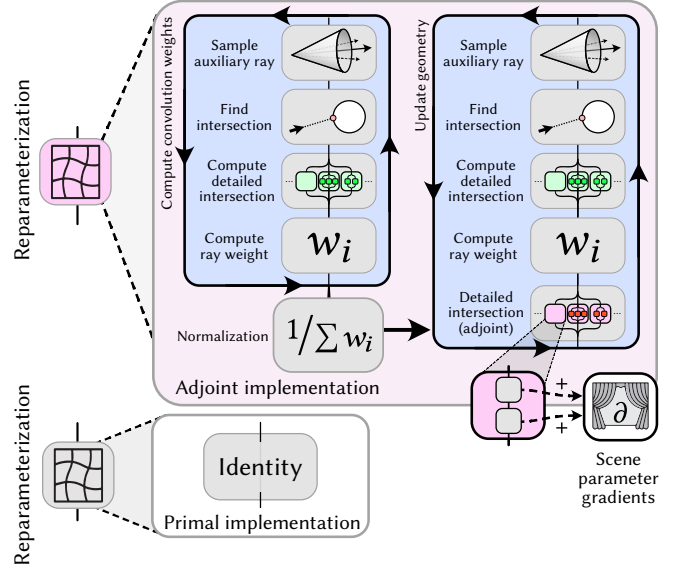


Fig. 13. To address the visibility-induced bias shown in Figure 12, rays must be *reparameterized* [Loubet et al. 2019]. In primal computation, reparameterizations have no effect and reduce to the identity. When differentiated, they trace auxiliary rays to construct a warp field [Bangaru et al. 2020] that counteracts silhouette motion. The reverse-mode derivative of this warp field scatters scene parameter gradients into intersected geometry.

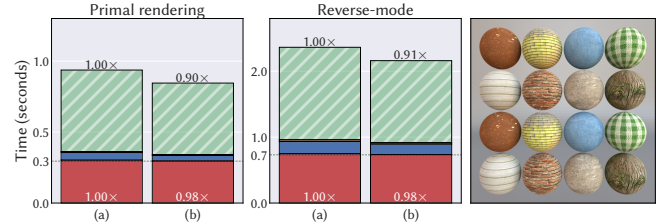


Fig. 14. Use of the GPU's native texture mapping units (TMUs) require extra steps to ensure differentiability. DR.JIT provides an operation named `dr.replace_grad(a, b)` that can be used to combine the hardware-accelerated lookup 'a' with the AD subgraph of a software-emulated lookup 'b' that never runs during primal evaluation. In a benchmark rendering of 16 spheres with 4K textures, we observe a small but measurable performance runtime improvement (on the order of 2-3%) when comparing (a) software-based (b) to hardware-accelerated lookups. Excising coordinate wrapping and interpolation operations from the kernel furthermore reduces compilation time by roughly 10%.

Figure 14 shows another application of this feature to perform differentiable texture lookups leveraging hardware-accelerated texture mapping units (TMUs) present on GPUs.

4.11 Results

We now present results showcasing the combination of differentiation and dynamic compilation. Note that we do not pursue complex applications scenarios involving inversion; our focus here is purely on the structure of the computation and the performance of the system on such differential workloads.

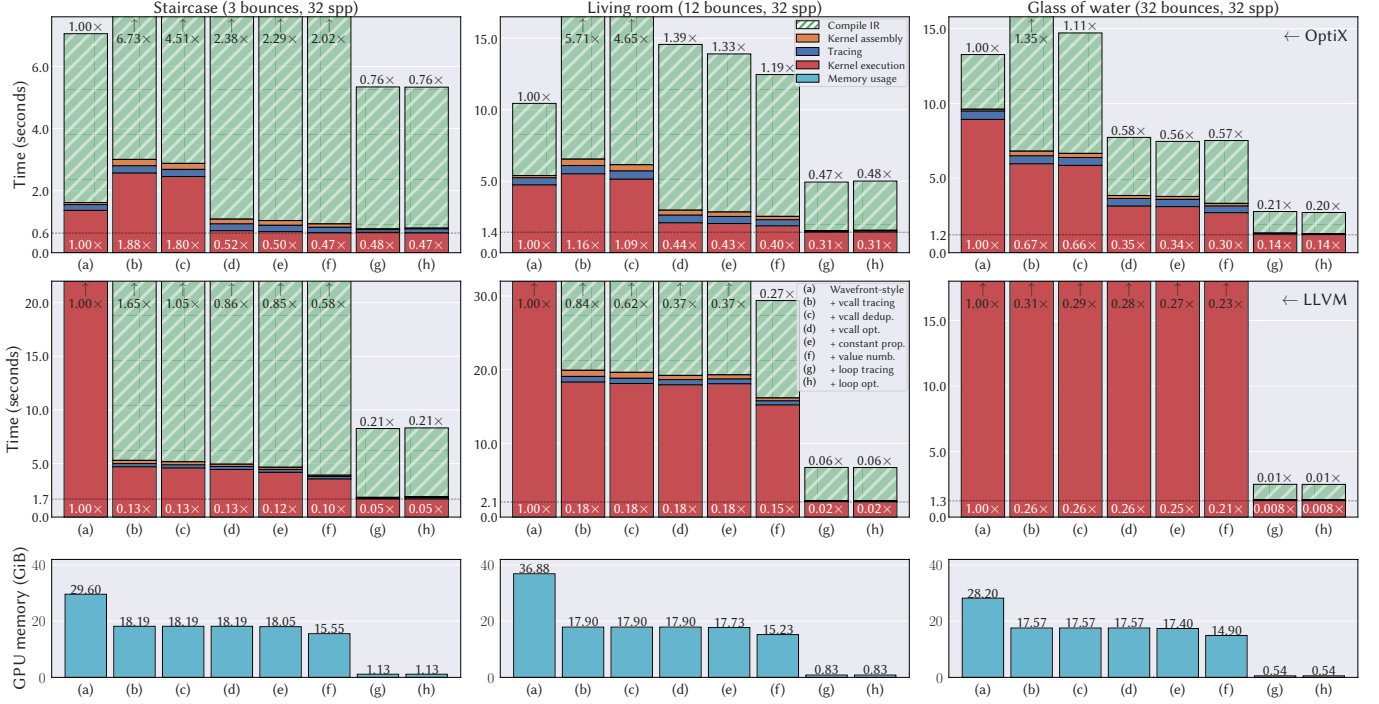


Fig. 15. Reverse-mode differentiation benchmark of *non-reparameterized* Path Replay Backpropagation analogous to Figure 7. We differentiate the rendered output of three scenes with respect to albedos and albedo textures, analyzing performance and the effect of different optimizations in DR.JIT. The rows show OptiX and LLVM runtime and peak memory usage (identical). Stacked bars indicate the time spent on backend IR compilation (hatched), kernel assembly (orange) and tracing (blue) within DR.JIT, as well as kernel execution (red). The wavefront baseline (a) on the left “unrolls” all use of loops and polymorphism into separate kernels that communicate through global memory. Going to the right, we successively enable (b) constant propagation, (c) compilation of polymorphism into subroutines, (d) subroutine deduplication, (e) optimization of polymorphic calls, (f) local value numbering, (g) loop tracing, and (h) loop optimizations.

Reverse-mode differentiation benchmark. Using the same set of scenes as before (*staircase*, *living room*, *glass of water*), we now use PRB to compute derivatives with respect to all albedo values (scalar, textured) as well as emitters like the environment map present in the *living room* scene. The information in Figure 15 only reflects the differential portion of a gradient step (i.e., phases #2 and #3 of the partition shown in Figure 10).

Many of the observations mirror our previous discussion of primal rendering in section 3.5. On the CPU, the benefit of megakernel-style evaluation continues to be dramatic, with speedups reaching $\sim 125\times$ compared to the baseline ($\sim 111\times$ in the primal benchmark).

One major change compared to the primal setting is that the computation must now evaluate the reverse-mode derivative of polymorphic calls. Consider the derivative of a function like BSDF evaluation that takes a large intersection record as input. Its derivative has even more inputs, and it additionally returns an output derivative for each primal input argument. Detecting and removing the resulting redundancies using global dead code elimination, constant propagation, and value numbering has a pronounced effect, with GPU speedups from this alone reaching $3.8\times$ in the *staircase* scene.

The differential megakernels enabled by the methods presented in this article consistently achieve the lowest tracing and kernel assembly time, lowest compilation time, and lowest runtime besides using a minimal amount of GPU memory. This last point becomes relevant

when optimizing large scene representations (e.g. 3D volumes) that consume most of the available device memory.

Reparameterized PRB benchmark. Figure 16 repeats this experiment once more, using *reparameterized PRB*. The introduction of reparameterizations and steps needed to evaluate the derivatives of adjacent vertices (Section 4.9) now leads to very large programs compared to primal rendering or non-reparameterized methods.

This time, we optimize the vertex positions of all scene geometry⁷. Again, this experiment produces no surprises and shows the effectiveness of the various optimizations. An interesting contrast between Figures 15 and 16 is the staircase-like sequence of bars in the latter, which clearly shows the benefit that each of the separate steps makes in both CUDA and especially the LLVM backend (which originally had a relatively flat profile in Figure 15). Once more, polymorphism-related optimizations are very important, with dead code elimination, value numbering, and constant propagation now producing a $7.4\times$ speedup on the OptiX backend.

The improvements of the loop state optimizations on runtime performance are relatively modest (runtime improvements of only a few percent in Figure 15), especially compared to some of the other steps. We believe that this optimization will play a more pronounced role in methods using *attached* Monte Carlo sampling [Zeltner et al.

⁷Derivatives will be biased in the *glass of water* scene containing dielectric objects. How to reparameterize through perfectly specular interfaces is an open research problem.

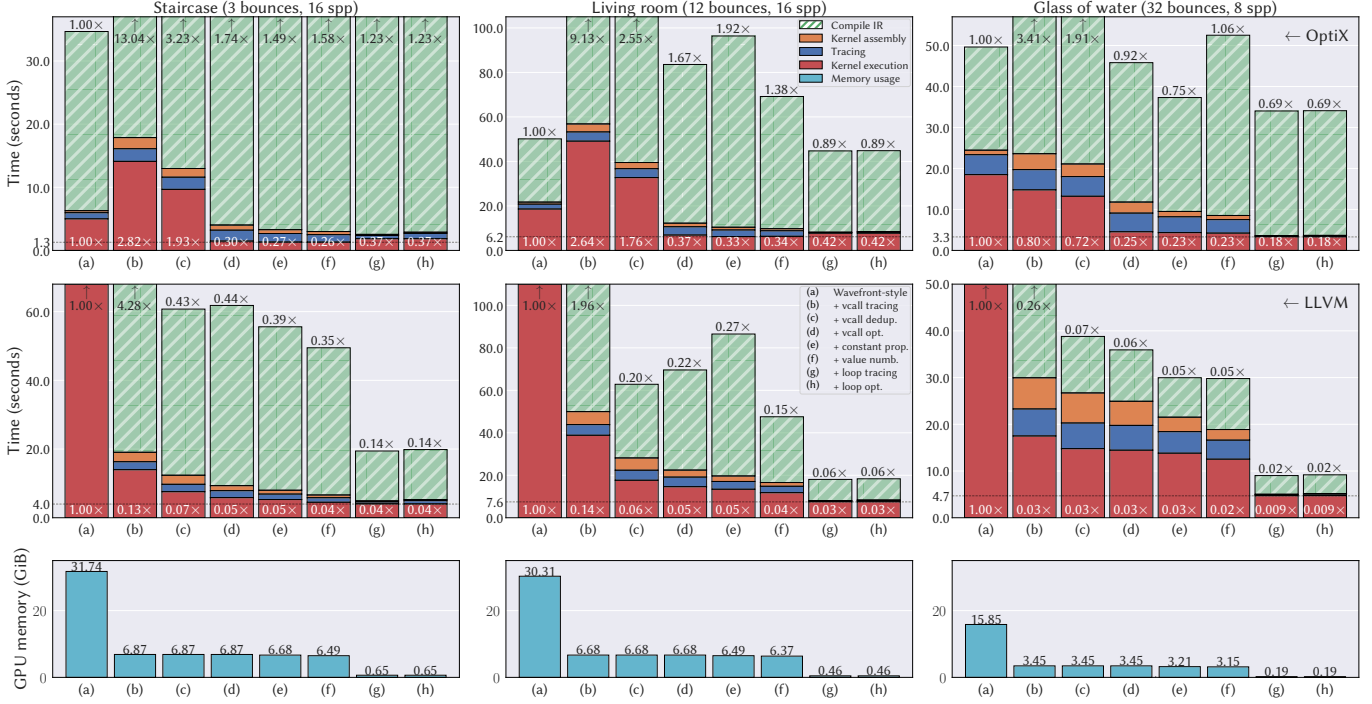


Fig. 16. Reverse-mode differentiation benchmark of *reparameterized* Path Replay Backpropagation analogous to Figures 7 and 15. Please see their captions for details on the visualization, and Section 4.11 for a discussion of this result.

2021; Vicini et al. 2021]), where large sets of derivatives must be exchanged between loop iterations.

Size reductions and size increases. Figure 17 provides another lens at the effect of our optimizations besides compilation and runtime performance. It shows that the majority of function arguments and return values are removed regardless of the application. In reverse-mode (reparameterized) PRB, the number of removed function outputs goes up significantly, as many computed derivatives have no effect. Reparameterized PRB carries a large amount of loop state to analyze the interaction between three adjacent path vertices; the implementation of this method was carefully optimized, which explains the smaller effect in the last row.

Table 1 gives an impression of how differentiation increases the size of a rendering algorithm, as measured in the number of compiled IR operations. The data indicates a relatively stable growth of 3–4× when going from primal path tracing to (differential) path replay. This is expected: besides steps for differentiation, the method runs two separate rendering passes. When reparameterizations are added on top, a different behavior emerges: wavefront evaluation produces significant ($> 30\times$) growth in the operation count, which our optimizations then stabilize to a factor of 7–8×.

Differentiating existing methods. DR.JIT can also differentiate rendering techniques that have not specifically been designed with this purpose in mind. Our last experiment does this with the builtin Mitsuba path tracer and contrasts its behavior to PRB. The path tracer contains a loop that DR.JIT handles using a checkpoint per scattering event (Section 4.3). Differentiable polymorphism can still

Primal	Subroutines (count)		130	269
	Subr. inputs (bytes)	600	← removed by optimization → 2181	
	Subr. outputs (bytes)	496	939	
	Loop state variables (bytes)	306	846	
PRB	Subroutines (count)		345	741
	Subr. inputs (bytes)	1876	6675	
	Subr. outputs (bytes)	976	3789	
	Loop state variables (bytes)	516	1596	
PRB reparam.	Subroutines (count)		1304	5087
	Subr. inputs (bytes)	10392	34679	
	Subr. outputs (bytes)	4688	24659	
	Loop state variables (bytes)	738	1158	

Fig. 17. Visualization of the total number of generated kernel subroutines, and the amount of data exchanged through function inputs, outputs, and loop state variables. The stated amounts are sums across the three benchmark scenes. Dashed bars indicate the proportion that is removed by the presented optimizations. The three rows showcase the differences in behavior when compiling primal rendering, PRB, and reparameterized PRB methods.

be used within each iteration, reducing memory usage and communication costs. Columns (a) and (b) show the performance of such an approach.

Differentiating with checkpoints is very memory-intensive. However, given a large supply of high-bandwidth memory (e.g. on the GPU), this approach can still yield good performance, since only

Table 1. Kernel sizes (measured in thousands of IR operations) averaged over the 3 benchmark scenes. This table provides numbers for primal rendering, reverse-mode PRB and reverse-mode reparameterized PRB, as well as the ratio relative to the primal column.

	Primal	PRB	(ratio)	Repa. PRB	(ratio)
wavefront	188.94	649.25	$\times 3.44$	6012.45	$\times 31.82$
+ vcall rec.	216.28	969.53	$\times 4.48$	6885.09	$\times 31.83$
+ vcall dedup.	141.21	654.49	$\times 4.63$	1042.37	$\times 7.38$
+ vcall opt.	138.74	495.65	$\times 3.57$	1103.82	$\times 7.96$
+ const prop.	127.13	448.29	$\times 3.53$	907.36	$\times 7.14$
+ value numb.	98.55	334.59	$\times 3.39$	800.07	$\times 8.12$
+ loop rec.	10.50	36.45	$\times 3.47$	78.77	$\times 7.50$
+ loop opt.	10.49	36.19	$\times 3.45$	78.69	$\times 7.50$

one rendering pass is needed (in comparison to PRB’s two passes). The runtime cost for PRB’s two-stage approach is initially higher in (c) (wavefront loop with polymorphism) but then drops to a competing or better level once compiled to a megakernel in (d). (These observations are consistent with the benchmarks reported in the original paper [Vicini et al. 2021].) Checkpointing becomes less competitive as an increasing numbers of scattering events are needed, for example in the case of participating media.

5 CONCLUSION

DR.JIT is a specialized compilation framework for physically based differentiable rendering algorithms, whose unique set of constraints makes their implementation using traditional means near-impossible. DR.JIT can trace large object-oriented codebases with polymorphic indirections, while providing fine-grained control over differentiation that is needed to leverage physical and mathematical symmetries. Clean abstractions can hide complex transformations like reparameterizations.

Its combination of tracing at JIT and AD levels is harmonious: by tracking the flow of primal and differential quantities at a global level, DR.JIT can specialize algorithms to the problem at hand, while discarding redundant computation. Its wavefront and megakernel implementations achieve excellent performance and run on diverse hardware architectures.

DR.JIT is not just meant to reproduce existing methods, but to provide a foundation for future research activities in this domain. We hope that it will lower the barrier to entry and enable new discoveries that push the boundaries of physically based differentiable rendering.

REFERENCES

- Apple, Inc. 2021. Metal Performance Shaders. <https://developer.apple.com/documentation/metalperformanceshaders/> (Accessed Jan 16, 2022).
- Sai Bangaru, Jesse Michel, Kevin Mu, Gilbert Bernstein, Tzu-Mao Li, and Jonathan Ragan-Kelley. 2021. Systematically Differentiating Parametric Discontinuities. *ACM Trans. Graph.* 40, 107 (2021).
- Sai Praveen Bangaru, Tzu-Mao Li, and Frédo Durand. 2020. Unbiased Warped-Area Sampling for Differentiable Rendering. *ACM Trans. Graph.* 39, 6 (nov 2020).
- Atilim Gunes Baydin, Barak A Pearlmutter, Alexey Andreyevich Radul, and Jeffrey Mark Siskind. 2018. Automatic differentiation in machine learning: a survey. *Journal of machine learning research* 18 (2018).
- Gilbert Louis Bernstein, Chinmayee Shah, Crystal Lemire, Zachary Devito, Matthew Fisher, Philip Levis, and Pat Hanrahan. 2016. Ebb: A DSL for Physical Simulation

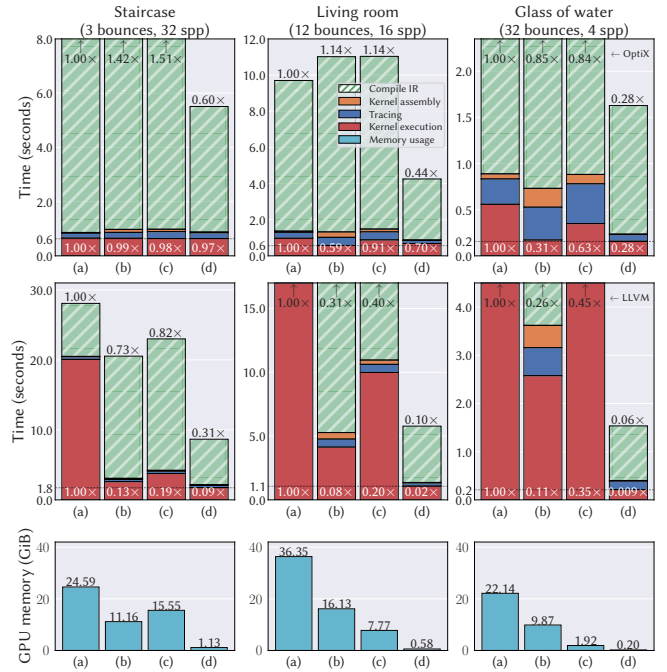


Fig. 18. Standard methods like path tracing can be differentiated within DR.JIT but require checkpointing. This figure compares the behavior of such a memory-intensive approach to a specialized PBDR method. (a) Reverse-mode differentiation of a standard path tracer in wavefront mode. (b) Path tracer with optimized polymorphic calls. (c) Wavefront PRB with optimized polymorphic calls. (d) PRB compiled to a megakernel.

- on CPUs and GPUs. *ACM Trans. Graph.* 35, 2 (may 2016).
- Christian Bischof, Alan Carle, George Corliss, Andreas Griewank, and Paul Hovland. 1992. ADIFOR—generating derivative codes from Fortran programs. *Scientific Programming* 1, 1 (1992).
- Benedikt Bitterli. 2016. *Rendering resources*. <https://benedikt-bitterli.me/resources/>.
- James Bradbury, Roy Frostig, Peter Hawkins, Matthew James Johnson, Chris Leary, Dougal Maclaurin, George Necula, Adam Paszke, Jake VanderPlas, Skye Wanderman-Milne, and Qiao Zhang. 2018. JAX: composable transformations of Python+NumPy programs. <http://github.com/google/jax>
- Ian Buck, Tim Foley, Daniel Horn, Jeremy Sugerman, Kayvon Fatahian, Mike Houston, and Pat Hanrahan. 2004. Brook for GPUs: stream computing on graphics hardware. *ACM transactions on graphics (TOG)* 23, 3 (2004).
- Brent Burley. 2012. Physically-based shading at Disney. In *ACM SIGGRAPH Talks*, Vol. 2012. vol. 2012.
- Brent Burley. 2015. Physically Based Shading in Theory and Practice: Extending the Disney BRDF to a BSDF with Integrated Subsurface Scattering. In *ACM SIGGRAPH 2015 Courses* (Los Angeles, California) (SIGGRAPH '15). Association for Computing Machinery, New York, NY, USA.
- Sharan Chetlur, Cliff Woolley, Philippe Vandermersch, Jonathan Cohen, John Tran, Bryan Catanzaro, and Evan Shelhamer. 2014. cuDNN: Efficient Primitives for Deep Learning. *CoRR abs/1410.0759* (2014). arXiv:1410.0759
- Luca Fascione, Johannes Hanika, Mark Leone, Marc Droske, Jorge Schwarzhaupt, Tomáš Davidovič, Andrea Weidlich, and Johannes Meng. 2018. Manuka: A batch-shading architecture for spectral path tracing in movie production. *ACM Transactions on Graphics (TOG)* 37, 3 (2018).
- Ioannis Gkioulekas, Anat Levin, and Todd Zickler. 2016. An evaluation of computational imaging techniques for heterogeneous inverse scattering. In *European Conference on Computer Vision*. Springer.
- Google. 2017. XLA: Optimizing Compiler for Machine Learning. <https://www.tensorflow.org/xla> (Accessed Jan 16, 2022).
- Andreas Griewank et al. 1989. On automatic differentiation. *Mathematical Programming: recent developments and applications* 6, 6 (1989).
- Andreas Griewank and Andrea Walther. 2008. *Evaluating derivatives: principles and techniques of algorithmic differentiation*. Vol. 105. SIAM.

- Pat Hanrahan and Jim Lawson. 1990. A language for shading and lighting calculations. In *Proceedings of the 17th annual conference on Computer graphics and interactive techniques*.
- Laurent Hascoet and Valérie Pascual. 2013. The Tapenade automatic differentiation tool: Principles, model, and specification. *ACM Transactions on Mathematical Software (TOMS)* 39, 3 (2013).
- Yong He, Kayvon Fatahalian, and Tim Foley. 2018. Slang: language mechanisms for extensible real-time shading systems. *ACM Transactions on Graphics (TOG)* 37, 4 (2018).
- Yong He, Tim Foley, and Kayvon Fatahalian. 2016. A system for rapid exploration of shader optimization choices. *ACM Transactions on Graphics (TOG)* 35, 4 (2016).
- Yuanming Hu, Luke Anderson, Tzu-Mao Li, Qi Sun, Nathan Carr, Jonathan Ragan-Kelley, and Frédo Durand. 2019a. DiffTaichi: Differentiable Programming for Physical Simulation. *arXiv preprint arXiv:1910.00935* (2019).
- Yuanming Hu, Tzu-Mao Li, Luke Anderson, Jonathan Ragan-Kelley, and Frédo Durand. 2019b. Taichi: A Language for High-Performance Computation on Spatially Sparse Data Structures. *ACM Trans. Graph.* 38, 6 (nov 2019).
- Michael Innes. 2019. Don't Unroll Adjoint: Differentiating SSA-Form Programs. *arXiv:1810.07951 [cs.PL]*
- Wenzel Jakob. 2019. Enoki: structured vectorization and differentiation on modern processor architectures. <https://github.com/mitsuba-renderer/enoki>. (Accessed: Jan 16, 2022).
- James T. Kajiya. 1986. The Rendering Equation. *SIGGRAPH Comput. Graph.* 20, 4 (aug 1986).
- Samuli Laine, Tero Karras, and Timo Aila. 2013. Megakernels considered harmful: Wavefront path tracing on GPUs. In *Proceedings of the 5th High-Performance Graphics Conference*.
- Chris Lattner and Vikram Adve. 2004. LLVM: A Compilation Framework for Lifelong Program Analysis and Transformation. San Jose, CA, USA.
- João Rui Leal and Brad Bell. 2017. *joaleal/CppADCodeGen: CppAD 2017*. <https://doi.org/10.5281/zenodo.836832>
- Mark Lee, Brian Green, Feng Xie, and Eric Tabellion. 2017. Vectorized production path tracing. In *Proceedings of High Performance Graphics*. ACM.
- Roland Leifä, Klaas Boesche, Sebastian Hack, Arsène Pérard-Gayot, Richard Membarth, Philipp Slusallek, André Müller, and Bertil Schmidt. 2018. AnyDSL: A Partial Evaluation Framework for Programming High-Performance Libraries. *Proceedings of the ACM on Programming Languages (PACMPL)* 2, OOPSLA (Nov. 2018).
- Tzu-Mao Li, Michaël Gharbi, Andrew Adams, Frédo Durand, and Jonathan Ragan-Kelley. 2018. Differentiable programming for image processing and deep learning in Halide. *ACM Transactions on Graphics (Proceedings of SIGGRAPH)* 37, 4 (2018).
- Seppo Linnainmaa. 1976. Taylor expansion of the accumulated rounding error. *BIT Numerical Mathematics* 16, 2 (1976).
- Guillaume Loubet, Nicolas Holzschuch, and Wenzel Jakob. 2019. Reparameterizing Discontinuous Integrands for Differentiable Rendering. *ACM Trans. Graph.* 38, 6 (nov 2019).
- William R Mark, R Steven Glanville, Kurt Akeley, and Mark J Kilgard. 2003. Cg: A system for programming graphics hardware in a C-like language. In *ACM SIGGRAPH 2003 Papers*.
- Michael McCool, Stefanus Du Toit, Tiberiu Popa, Bryan Chan, and Kevin Moule. 2004. Shader Algebra. *ACM Trans. Graph.* 23, 3 (aug 2004).
- Michael D McCool, Zheng Qin, and Tiberiu S Popa. 2002. Shader metaprogramming. In *Proceedings of the ACM SIGGRAPH/EUROGRAPHICS conference on Graphics hardware*.
- William S Moses and Valentin Churavy. 2020. Instead of Rewriting Foreign Code for Machine Learning, Automatically Synthesize Fast Gradients. *arXiv preprint arXiv:2010.01709* (2020).
- William S Moses, Valentin Churavy, Ludger Paehler, Jan Hüchelheim, Sri Hari Krishna Narayanan, Michel Schanen, and Johannes Doerfert. 2021. Reverse-mode automatic differentiation and optimization of GPU kernels via enzyme. In *Proceedings of the International Conference for High Performance Computing, Networking, Storage and Analysis*.
- Merlin Nimier-David, Sébastien Speierer, Benoît Ruiz, and Wenzel Jakob. 2020. Radiative Backpropagation: An Adjoint Method for Lightning-Fast Differentiable Rendering. *ACM Trans. Graph.* 39, 4 (jul 2020).
- Merlin Nimier-David, Delio Vicini, Tizian Zeltner, and Wenzel Jakob. 2019. Mitsuba 2: A Retargetable Forward and Inverse Renderer. *ACM Trans. Graph.* 38, 6 (nov 2019).
- John F Nolan. 1953. *Analytical differentiation on a digital computer*. Ph.D. Dissertation. Massachusetts Institute of Technology.
- Melissa E. O'Neill. 2014. *PCG: A Family of Simple Fast Space-Efficient Statistically Good Algorithms for Random Number Generation*. Technical Report HMC-CS-2014-0905. Harvey Mudd College, Claremont, CA.
- Steven G. Parker, James Bigler, Andreas Dietrich, Heiko Friedrich, Jared Hoberock, David Luebke, David McAllister, Morgan McGuire, Keith Morley, Austin Robison, and Martin Stich. 2010. OptiX: A General Purpose Ray Tracing Engine. *ACM Trans. Graph.* 29, 4 (jul 2010).
- Adam Paszke, Sam Gross, Soumith Chintala, Gregory Chanan, Edward Yang, Zachary DeVito, Zeming Lin, Alban Desmaison, Luca Antiga, and Adam Lerer. 2017. Automatic differentiation in PyTorch. (2017).
- Barak A Pearlmutter and Jeffrey Mark Siskind. 2008. Reverse-mode AD in a functional framework: Lambda the ultimate backpropagator. *ACM Transactions on Programming Languages and Systems (TOPLAS)* 30, 2 (2008).
- Matt Pharr, Wenzel Jakob, and Greg Humphreys. 2020. *Implementation of the forthcoming 4th edition of Physically Based Rendering: From Theory to Implementation*. <https://github.com/mmp/pbrt-v4>
- Matt Pharr and William R Mark. 2012. ispc: A SPMD compiler for high-performance CPU programming. In *2012 Innovative Parallel Computing (InPar)*. IEEE.
- Lev Semenovich Pontryagin. 1962. *Mathematical theory of optimal processes*. CRC Press.
- Arsène Pérard-Gayot, Richard Membarth, Roland Leifä, Sebastian Hack, and Philipp Slusallek. 2019. Rodent: Generating Renderers without Writing a Generator. *ACM Transactions on Graphics* 38, 4 (7 2019).
- Jonathan Ragan-Kelley, Connelly Barnes, Andrew Adams, Sylvain Paris, Frédo Durand, and Saman Amarasinghe. 2013. Halide: A Language and Compiler for Optimizing Parallelism, Locality, and Recomputation in Image Processing Pipelines. *SIGPLAN Notices* 48, 6 (June 2013).
- Jeffrey Mark Siskind and Barak A Pearlmutter. 2018. Divide-and-conquer checkpointing for arbitrary programs with no user annotation. *Optimization Methods and Software* 33, 4-6 (2018).
- Bert Speelpenning. 1980. *Compiling fast partial derivatives of functions given by algorithms*. Ph.D. Dissertation. University of Illinois at Urbana-Champaign.
- Delio Vicini, Sébastien Speierer, and Wenzel Jakob. 2021. Path Replay Backpropagation: Differentiating Light Paths Using Constant Memory and Linear Time. *ACM Trans. Graph.* 40, 4 (jul 2021).
- Yu M Volin and GM Ostrovskii. 1985. Automatic computation of derivatives with the use of the multilevel differentiating technique—1. algorithmic basis. *Computers & mathematics with applications* 11, 11 (1985).
- Ingo Wald, Sven Woop, Carsten Benthin, Gregory S. Johnson, and Manfred Ernst. 2014. Embree: A Kernel Framework for Efficient CPU Ray Tracing. *ACM Transactions on Graphics* 33, 4 (July 2014).
- Robert Edwin Wengert. 1964. A simple automatic derivative evaluation program. *Commun. ACM* 7, 8 (1964).
- Tizian Zeltner, Sébastien Speierer, Iliyan Georgiev, and Wenzel Jakob. 2021. Monte Carlo Estimators for Differential Light Transport. *Transactions on Graphics (Proceedings of SIGGRAPH)* 40, 4 (Aug. 2021). <https://doi.org/10.1145/3450626.3459807>